CANCER IMMUNOLOGY

CD5 deletion enhances the antitumor activity of adoptive T cell therapies

**Ruchi P. Patel[1,2,3], Guido Ghilardi[1,2,3], Yunlin Zhang[1,2,3], Yi-Hao Chiang[1,4], Wei Xie[1,5], Puneeth Guruprasad[1,2,3], Ki Hyun Kim[1,2,3], Inkook Chun[1,2,3], Mathew G. Angelos[1,2,3], Raymone Pajarillo[1,2,3], Seok Jae Hong[1,2,3], Yong Gu Lee[1,2,3,6], Olga Shestova[1,2], Carolyn Shaw[1], Ivan Cohen[1,2,3], Aasha Gupta[1,2,3], Trang Vu[7], Dean Qian[7], Steven Yang[7], Aditya Nimmagadda[7], Adam E. Snook[7], Nicholas Siciliano[7], Antonia Rotolo[1], Arati Inamdar[8], Jaryse Harris[8], Ositadimma Ugwuanyi[1,2,3], Michael Wang[1,2,3], Alberto Carturan[1,2,3], Luca Paruzzo[1,2,3], Linhui Chen[1,2,3], Hatcher J. Ballard[2,3], Tatiana Blanchard[1], Chong Xu[1], Mohamed Abdel-Mohsen[9], Khatuna Gabunia[1], Maria Wysocka[10], Gerald P. Linette[1], Beatriz Carreno[1], David M. Barrett[1,11], David T. Teachey[11], Avery D. Posey[1], Daniel J. Powell Jr.[1,8], C. Tor Sauter[1,2,3], Stefano Pileri[12], Vinodh Pillai[13], John Scholler[1], Alain H. Rook[10], Stephen J. Schuster[1,2,3], Stefan K. Barta[1,2,3], Patrizia Porazzi[1,2,3], Marco Ruella[1,2,3]*

Most patients treated with US Food and Drug Administration (FDA)–approved chimeric antigen receptor (CAR) T cells eventually experience disease progression. Furthermore, CAR T cells have not been curative against solid cancers and several hematological malignancies such as T cell lymphomas, which have very poor prognoses. One of the main barriers to the clinical success of adoptive T cell immunotherapies is CAR T cell dysfunction and lack of expansion and/or persistence after infusion. In this study, we found that CD5 inhibits CAR T cell activation and that knockout (KO) of CD5 using CRISPR-Cas9 enhances the antitumor effect of CAR T cells in multiple hematological and solid cancer models. Mechanistically, CD5 KO drives increased T cell effector function with enhanced cytotoxicity, in vivo expansion, and persistence, without apparent toxicity in preclinical models. These findings indicate that CD5 is a critical inhibitor of T cell function and a potential clinical target for enhancing T cell therapies.

INTRODUCTION

Adoptive T cell therapy (ACT) and, specifically, chimeric antigen receptor (CAR T) therapy have led to unprecedented clinical responses in relapsed or refractory (r/r) B cell acute lymphoblastic leukemia (B-ALL), non-Hodgkin's lymphoma (NHL), and multiple myeloma (*1*–*3*). Despite these results, most patients treated with CAR T either do not respond or eventually relapse (*4*–*10*). Moreover, CAR T therapy has not yet demonstrated significant responses in solid cancers (*11*) and in several hematological malignancies, such as T cell lymphoma (TCL)/acute lymphoblastic leukemia (T-ALL) and others (*12*–*15*). Thus, there is a dire need to enhance the currently available CAR T products and extend this effective approach to successfully treat more types of cancer.

One of the main barriers to the clinical success of adoptive T cell immunotherapies is suboptimal T cell activation and a lack of persistence after infusion because of T cell dysfunction (*16*). Therefore, reducing the inhibition of CAR activation will likely amplify the efficacy of adoptive T cell immunotherapy. To this end, we studied the cysteine-rich scavenger receptor, CD5. CD5 associates with the T cell receptor (TCR) complex and inhibits its activation through several mediators, including SHP1, CBL, and CBL-B (*17*). It has been shown that tumor-specific T cells can undergo a rapid intratumoral adaptation process by down-regulating the expression of CD5 to enhance TCR signaling (*18*, *19*). Moreover, an increase in CD5 expression has been observed in peripheral anergic $CD8^+$ T cells chronically exposed to antigens (*20*). CD5-deficient mice showed improved B16 melanoma tumor control compared with wild-type mice (*21*). Previous studies have evaluated CD5 deletion as a strategy to avoid fratricide in CAR T cells against CD5 itself (*22*) because CD5 is expressed in normal T cells. However, genetically deleting CD5 in adoptively transferred T cells has not been studied as a strategy to enhance other T cell–based therapies, and the mechanism of CD5 inhibition in CAR T is not known. In this study, we tested CD5 knockout (KO) in CAR and TCR T cells against multiple models of hematological malignancies and solid cancers. We observed a marked enhancement of the antitumor effect of the adoptively transferred T cells, which was associated with enhanced expansion and persistence. The antitumor effect observed here surpasses that of programmed cell death protein 1 (PD-1) KO, which is presently the most frequently targeted gene deletion in ongoing clinical trials. Mechanistically, we observed RNA up-regulation of T cell activation–related pathways in CD5 KO CAR T cells and enhanced expression of cytotoxic machinery genes. In conclusion, we demonstrated that CD5 is a key negative regulator of CAR T cells and is a potential immune checkpoint for adoptive T cell immunotherapies.

[1]Center for Cellular Immunotherapies, University of Pennsylvania, Philadelphia, PA, USA. [2]Division of Hematology and Oncology, Hospital of University of Pennsylvania, Philadelphia, PA, USA. [3]Lymphoma Program, Abramson Cancer Center, University of Pennsylvania, Philadelphia, PA, USA. [4]Division of Hematology and Oncology, MacKay Memorial Hospital, Taipei, Taiwan. [5]Institute of Hematology, Union Hospital, Tongji Medical College, Huazhong University of Science and Technology, Wuhan, China. [6]College of Pharmacy and Institute of Pharmaceutical Science and Technology, Hanyang University, Ansan, Republic of Korea. [7]viTToria Biotherapeutics, Philadelphia, PA, USA. [8]Department of Pathology and Laboratory Medicine, Perelman School of Medicine at University of Pennsylvania, Philadelphia, PA, USA. [9]Vaccine and Immunotherapy Center, Wistar Institute, Philadelphia, PA, USA. [10]Department of Dermatology, Perelman School of Medicine at University of Pennsylvania, Philadelphia, PA, USA. [11]Division of Oncology, Children's Hospital of Philadelphia, PA, USA. [12]Division of Haematopathology, Istituto Europeo di Oncologia IRCCS, Italy. [13]Division of Hemato-pathology, Children's Hospital of Philadelphia, Philadelphia, PA, USA.
*Corresponding author. Email: mruella@upenn.edu

RESULTS

CRISPR-Cas9 CD5 KO enhances the antitumor activity of CAR T cells against CD5$^+$ tumors

We initially tested the role of CD5 KO in CAR T cells against T cell neoplasms because there are no US Food and Drug Administration (FDA)–approved CAR T therapies for this orphan disease (*15*). CD5 is a T cell neoplasm target that is highly and homogeneously expressed in about 85% of patients with TCL and T-ALL (fig. S1, A and B). In this cancer model of anti-CD5 CAR T cells for TCLs, we speculated that the deletion of CD5, in addition to reducing T cell inhibition, would also avoid CAR T–T cell fratricide because CD5 is expressed in normal T cells.

We first aimed to select a lead CRISPR-Cas9 guide RNA (gRNA) to delete *CD5* in CAR T cells. We designed and screened eight single gRNAs targeting *CD5* and then selected the most efficient, sgRNA #4, on the basis of protein expression analyses (flow cytometry and protein immunoblot; fig. S1, C and D, and table S1). We used sgRNA #4 to knock out *CD5* in primary T cells using an optimized CAR T manufacturing process that included Cas9-sgRNA electroporation on day 0, followed by anti-CD3/CD28 bead activation on day 1, lentiviral transduction on day 2, and harvest at day >15 based on cell size (Fig. 1A). CD5 deletion was reproducibly efficient (>90% protein KO efficiency) by protein analyses (Fig. 1B and fig. S1D). We then used an optimized anti-CD5 CAR construct derived from the 17-antibody clone (*23*), which exhibited both high affinity and specificity for a membrane-proximal CD5 epitope. Once we established a platform to efficiently knock out CD5 in CAR T cells and cloned an optimal anti-CD5 CAR, we investigated the effect of CD5 KO in CAR T cells by comparing CD5 KO CART5 cells with mock electroporated CART5 cells [CD5 wild-type (WT) CART5 = mock KO CART5; Fig. 1C].

During manufacturing, the growth rate of mock KO CART5 cells was reduced compared with CD5 KO CART5 cells (Fig. 1D; mock KO CART5 versus CD5 KO CART5, $P = 0.07$ on day 17), suggesting a degree of fratricide that, although notable, did not completely halt their expansion; therefore, we hypothesized that there were additional mechanisms protecting the cells from overt fratricide. CAR expression in mock KO CART5 cells was similar to that of CD5 KO CART5 cells (Fig. 1E and fig. S2A). Furthermore, mock KO untransduced (UTD) cells showed a similar percentage of CD5 in comparison with mock KO CART5 cells (Fig. 1B; fig. S2A); however, there was a reduction in the mean fluorescence intensity (MFI) of CD5 between the mock KO UTD and mock KO CART5 cells (Fig. 1B). When we analyzed CD5 expression in T cells at several time points during manufacturing, we found that CAR5 transduction correlated with a decrease in CD5 expression (fig. S2B). In addition, epitope masking (*24*) was observed in mock KO CART5 cells (fig. S2C), which was further validated by the result that CD5$^+$ Jurkat cells transduced with CAR5 (Jurkat-CAR5) were resistant to CART5-induced killing despite having CD5 on their surface (fig. S2D). These studies suggest that mock CART5 cells do not experience complete fratricide because of a combination of both CD5 protein down-regulation and CD5:CAR5 in cis engagement on the surface (epitope masking).

However, at the end of manufacturing, CD5 KO CART5 cells were enriched in naïve T cells when compared with mock KO CART5 cells and had lower effector memory T cells (Fig. 1F). Moreover, CD5 KO CART5 cells presented lower expression of exhaustion markers such as PD-1 and LAG-3 in CD8$^+$ T cells and a trend of less CD39 and TIM3 in CD4$^+$ T cells as compared with mock KO CART5 cells (Fig. 1G and fig. S2, E and F). These data demonstrate that the removal of CD5 during manufacturing leads to a final product that is less differentiated and exhausted because of the reduction of CAR T–T cell fratricide. We then evaluated the efficacy of CD5 KO versus mock KO CART5 cells in vitro against CD5$^+$ and CD5$^-$ cancer cells. Both mock KO CART5 and CD5 KO CART5 cells were highly effective in killing CD5$^+$ primary TCL (Sézary cells), primary T-ALL, and Jurkat cell lines in vitro but demonstrated no cytotoxic effects against the CD5$^-$ B-ALL cell line Nalm6 (Fig. 2A and fig. S2G). However, enhanced proliferation was observed in CD5 KO CART5 cells as compared with mock KO CART5 cells, as shown by increased dilution of CellTrace Violet upon target-specific stimulation of irradiated Jurkat cells (Fig. 2B). To evaluate the in vivo efficacy of CD5 KO CART5 cells, we engrafted NOD-SCID gamma chain–deficient (NSG) mice with Jurkat cells and randomized them to receive CD5 KO CART5, mock KO CART5, or UTD controls (Fig. 2C). We observed that CD5 KO CART5 cells markedly increased tumor control over UTD groups and mock KO CART5 cells. Accordingly, overall survival was significantly longer in the CD5 KO CART5 group when compared with the mock KO CART5 group (median overall survival for mock KO CART5 = 55 days versus CD5 KO CART5 = undefined; $P = 0.0062$, Mantel-Cox; Fig. 2, C and D). This enhanced antitumor effect was associated with significantly increased T cell expansion in the peripheral blood of CD5 KO CART5–treated mice as compared with controls, and the persistence of CD5 KO CART5 cells was also longer than that of controls (Fig. 2E). Last, we confirmed these results using a patient-derived xenograft (PDX) model of primary T-ALL (TH20). In this model, CD5 KO CART5 cells showed significantly increased tumor control and overall survival (median overall survival for mock KO CART5 = 68 days versus CD5 KO CART5 = undefined; $P = 0.0007$, Mantel-Cox) compared with mock KO CART5 cells (Fig. 2, F and G), further confirming that CRISPR-Cas9 deletion of CD5 in CART5 cells could serve as an effective agent for treating T cell neoplasms.

CAR T cells against B cell lymphoid malignancies display improved efficacy with CD5 deletion

CD5 KO led to a marked increase in the in vivo ability of CD5 KO CART5 cells to expand, persist, and control tumor growth. However, in the CART5 model, this effect could have been mediated predominantly by the prevention of CAR T–T cell fratricide. To study the effect of CD5 KO in CAR T function without the possible confounder of CAR T–T cell fratricide, we knocked out CD5 in CART19 cells manufactured using an FDA-approved CAR19–4-1BBz construct (tisagenlecleucel) and tested its function against CD19$^+$ leukemia and lymphoma models. Control AAVS1 KO CART19 cells showed comparable killing efficacy as compared with mock KO CART19 cells, suggesting that the gRNA per se does not affect CAR T cell function (fig. S3A). Although similar phenotypes were observed in mock KO and CD5 KO CART19 cells at the end of manufacturing (fig. S3, B to F), we observed enhanced activation (fig. S3G) and antitumor effects of CD5 KO CART19 cells in vivo in xenograft models (Fig. 3, A to C). In a B-ALL (Nalm6) model, NSG mice treated with CD5 KO CART19 cells showed improved tumor control compared with the mock KO CART19 group (Fig. 3A). This increased tumor control correlated with significantly prolonged survival in mice treated with CD5 KO CART19 cells (median overall survival for mock KO CART19 = 37 days versus CD5 KO CAR T19 = 67.5 days;

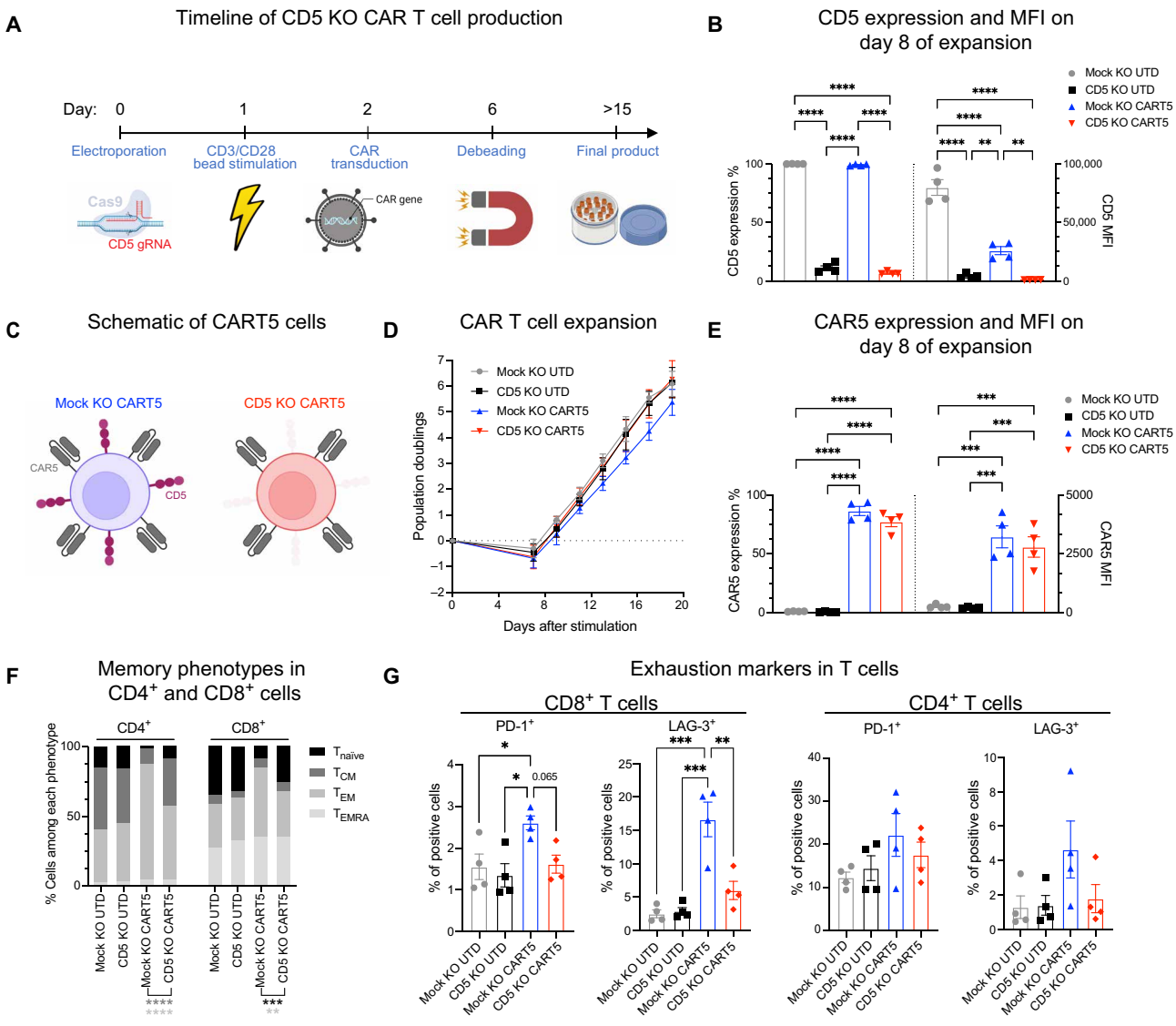

Fig. 1. CD5 KO enhances CART5 phenotype as compared with mock KO CART5 cells. (**A**) CD5 KO CAR T expansion protocol. (**B**) Representative bar graph showing expression of CD5 on the groups of engineered T cells on day 8 of expansion and representative bar graph showing MFI of CD5 on the same cells. $n = 2$ donors, two technical replicates. (**C**) Schematic of mock KO and CD5 KO CART5 cells. (**D**) Expansion of bead-stimulated T cells shown in population doublings (log_2-transformed fold change of total cell counts). $n = 4$ donors. (**E**) Representative bar graph showing the expression of CAR5 on the groups of engineered T cells on day 8 of expansion and representative bar graph showing MFI of CAR5 on the same cells. $n = 2$ donors, two technical replicates. (**F**) T cell memory phenotypes of each engineered T cell groups at the end of expansion. $T_{naïve}$, naïve T cells, $CD45RA^+CCR7^+$; T_{CM}, central memory T cells, $CD45RA^-CCR7^+$; T_{EM}, effector memory T cells, $CD45RA^-CCR7^-$; T_{EMRA}, effector memory T cells reexpressing CD45RA, $CD45RA^+CCR7^-$. $n = 4$ donors. (**G**) Expression of T cell exhaustion markers PD-1 and LAG-3 on each engineered T cell group at the end of expansion in $CD8^+$ and $CD4^+$ cells. $n = 4$ donors. One-way ANOVA was performed with Tukey correction for multiple comparisons; $^*P < 0.05$, $^{**}P < 0.01$, $^{***}P < 0.001$, and $^{****}P < 0.0001$.

$P = 0.0292$, Mantel-Cox; Fig. 3B). As observed in the CART5 model, increased numbers of T cells were observed in the peripheral blood of CD5 KO CART19–treated mice (Fig. 3C). To evaluate the capacity of CD5 KO CART19 cells to establish long-term immune memory, mice were rechallenged in a separate experiment with the same tumor (day 21, 1×10^6 Nalm6). None of the mice treated with CD5 KO CART19 cells exhibited tumor engraftment, unlike a few mice treated with mock KO CART19 cells, indicating the ability of CD5 KO CART19 cells to establish immunological memory in these models (fig. S4A).

We further tested the ability of CD5 KO to enhance the killing of the $CD30^+$ Hodgkin's lymphoma cell line HDLM2 (*25*). Cancer cells were treated with CAR T cells for 72 hours, and cytotoxicity was measured by comparing cell growth with a UTD control group. As expected, there was a marked improvement in the effectiveness of CD5 KO CART30 at lower effector:target (E:T) ratios (0.125:1 and 0.25:1), which act as "stress tests." Conversely, at higher E:T ratios, the tumor was effectively cleared in all CAR T groups, thus eliminating the potential of observing any discernible differences (fig. S4B). To corroborate the significance of the in vitro findings, we also

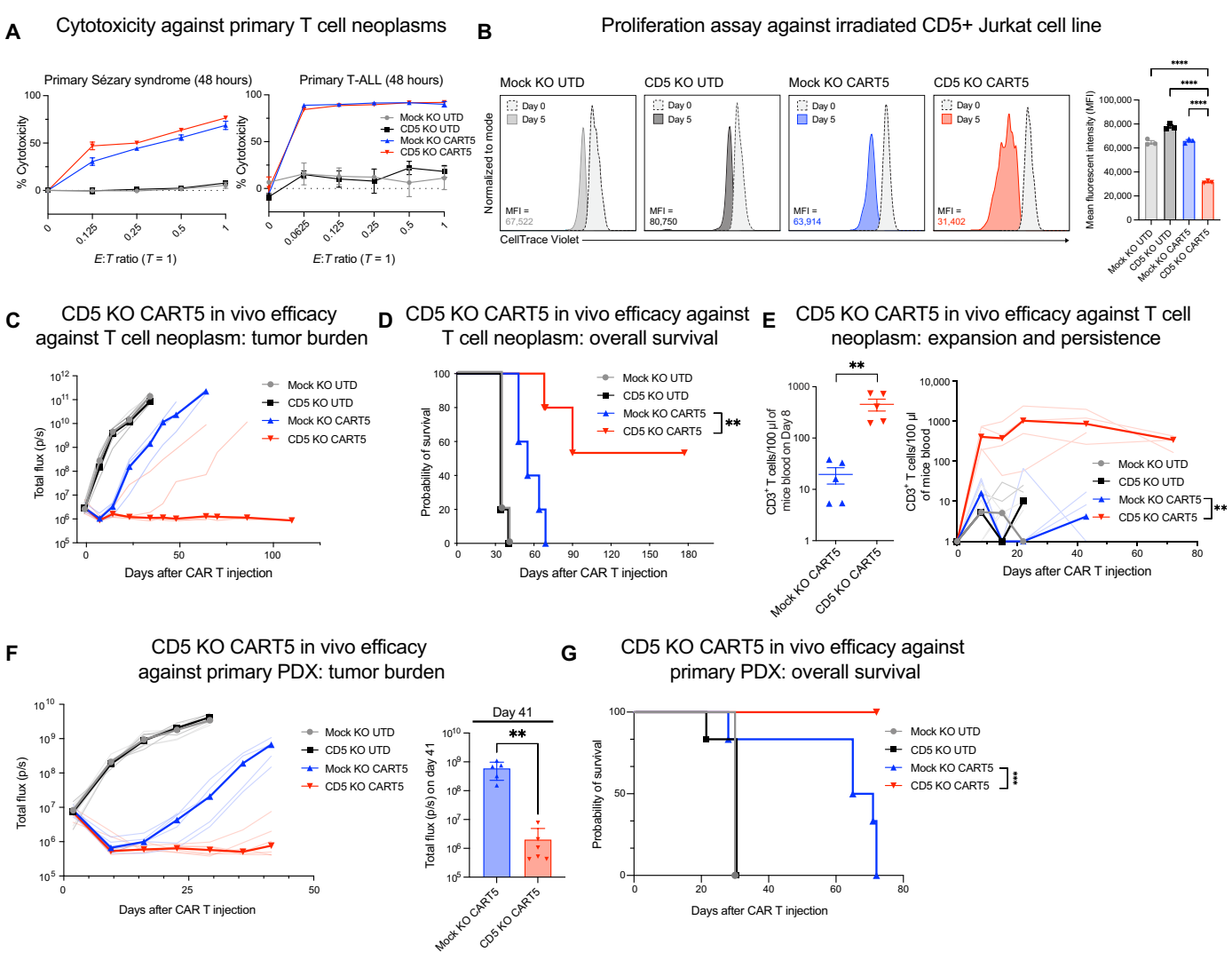

Fig. 2. CD5 KO in CART5 T cells improves engineered T cell product compared with mock KO CART5 cells. (**A**) Percent cytotoxicity of UTD or CART5 cells against CD5$^+$ primary Sézary or primary T-ALL cells after 48 hours. (**B**) UTD and CART5 cells labeled with CellTrace Violet were cocultured with irradiated Jurkat cell line at a 1:1 E:T ratio for 5 days. Left: Representative flow cytometry histograms. Right: Compilation of MFI of three technical replicates. Representative data of two independent experiments are shown. (**C**) NSG mice were engrafted with 1×10^6 Jurkat cells (intravenously) on day −7 and randomized to receive 1×10^6 CD5 KO CART5 or mock KO CART5 cells or an equivalent number of UTD controls (intravenously) on day 0. Bioluminescence imaging of tumor burden in each NSG mouse ($n = 5$ mice per group) engrafted with Jurkat cell line. The bolded line represents the median of each group. Representative data of two independent experiments are shown. (**D**) The survival rate of each treatment group in xenograft T cell neoplasm model is shown in a Kaplan-Meier survival curve. (**E**) Left: Absolute cell counts of hCD3$^+$ T cells in 100 µl of mouse blood at day 8. Right: Absolute cell counts of hCD3$^+$ T cells in 100 µl of mouse blood over time. The bolded line represents the median of each group. (**F**) NSG mice were engrafted with 1×10^6 TH20 cells on day −7 (intravenously) and randomized to receive 1×10^6 CD5 KO CART5 cells, mock KO CART5 cells, or UTD controls (intravenously) on day 0. Left: Bioluminescence imaging of tumor burden in each NSG mouse ($n = 5$ or 6 mice per group) engrafted with primary PDX cells. The bolded line represents the median of each group. Right: Bioluminescence flux of tumor burden of mice treated with mock KO CART5 cells or CD5 KO CART5 cells on day 41. (**G**) The survival rate of each treatment group in primary PDX model is shown in a Kaplan-Meier survival curve. Student's *t* test was used to compare two groups; in analyses where multiple groups were compared, one-way ANOVA was performed with Tukey correction. Survival curves were compared using the log-rank (Mantel-Cox) test. $^{**}P < 0.01$, $^{***}P < 0.001$, and $^{****}P < 0.0001$.

performed an in vivo experiment in which CD5 KO CART30 cells demonstrated stronger tumor control against HDLM2 than both mock KO UTD and mock KO CART30 cells (Fig. 3D).

Deletion of CD5 results in strong responses in adoptive T cell therapy against solid cancers

We speculated that CD5 KO could also enhance CAR T therapies against solid cancers. CAR T for solid cancers has been mostly unsuccessful because of a lack of proliferation and persistence (*26*). We initially tested CD5 KO CAR T cells in a model of pancreatic ductal cancer adenocarcinoma (PDAC; AsPC1 cell line). We deleted CD5 in anti-mesothelin CAR T cells (CARTmeso) using a clinically relevant CAR construct (M5 clone) previously used in the clinic (NCT03054298) (*27*). We used both a late relapse model (high T cell dose, 0.75×10^6 CAR$^+$ cells) and a primary failure model (low T cell dose, 0.2×10^6 CAR$^+$ cells) to test the effect of CD5 KO on CAR T efficacy. In the late relapse model, which included higher T cell numbers, CD5 KO CAR T cells displayed enhanced tumor control

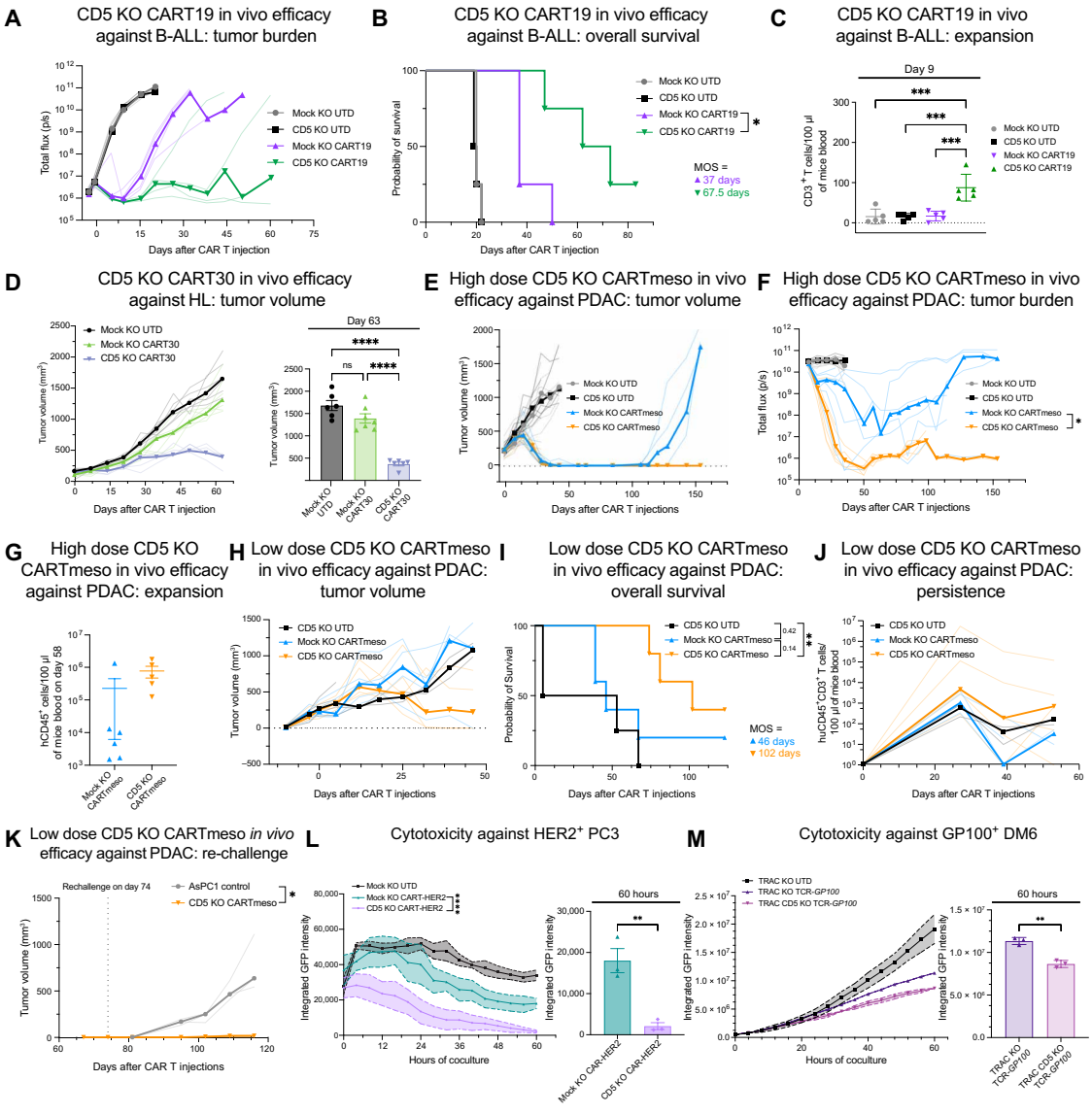

Fig. 3. CD5 KO enhances CART19 therapy in B-ALL and CARTmeso therapy in solid tumor model of pancreatic ductal adenocarcinoma. (**A**) NSG mice were engrafted with 1×10^6 Nalm6 cells (intravenous) on day −5 and injected with 1×10^6 mock or CD5 KO CART19 cells (intravenous) on day 0. Bioluminescence imaging of tumor burden in each NSG mouse ($n = 4$ mice per group) engrafted with Nalm6 B-ALL cell line. The bolded line represents the median of each group. Representative data of two independent experiments are shown. (**B**) The survival rate of each treatment group in xenograft B-ALL model is shown in a Kaplan-Meier survival curve. (**C**) NSG mice ($n = 5$ mice per group) were engrafted with 1×10^6 Nalm6 cells (intravenously) on day −6 and injected with 1×10^6 mock or CD5 KO CART19 cells (intravenously) on day 0. Absolute cell counts of hCD3$^+$ T cells in 100 µl of mouse blood at day 9. (**D**) NSG mice were engrafted with 15×10^6 HDLM2 HL cells (subcutaneously) on day −62 and injected with 0.25×10^6 mock or CD5 KO CART30 cells (intravenously) on day 0. Left: Tumor volume (in mm^3) in each NSG mouse ($n = 6$ or 7 mice per group) engrafted with HDLM2 HL cell line. The bolded line represents the median of each group. Right: Tumor volume of mice on day 63. (**E**) NSG mice were engrafted with 2×10^6 AsPC1 cells (subcutaneously) on day −27 and injected with 0.75×10^6 mock or CD5 KO CARTmeso cells (intravenously) on day 0. Tumor volume (in mm^3) in each NSG mouse ($n = 7$ mice per group) engrafted with AsPC1 PDAC cell line. The bolded line represents the median of each group. Representative data of two independent experiments are shown. (**F**) Bioluminescence imaging of tumor burden in each NSG mouse. The bolded line represents the median of each group. (**G**) Absolute cell counts of hCD45$^+$ T cells in 100 µl of mouse blood at day 58. (**H**) NSG mice were engrafted with 2×10^6 AsPC1 PDAC cells (subcutaneously) on day −23 and injected with 0.2×10^6 mock or CD5 KO CARTmeso cells (intravenously) on day 0. Tumor volume (in mm^3) in each NSG mouse ($n = 4$ or 5 mice per group) engrafted with AsPC1 PDAC cell line. The bolded line represents the median of each group. (**I**) The survival rate of each treatment group in xenograft PDAC model is shown in a Kaplan-Meier survival curve. (**J**) Absolute cell counts of hCD45$^+$ hCD3$^+$ T cells in 100 µl of mouse blood over time. The bolded line represents the median of each group. (**K**) Tumor volume (in mm^3) in control NSG mice ($n = 3$) or mice treated with CD5 KO CARTmeso ($n = 2$) and rechallenged with AsPC1 cells on day 74. The bolded line represents the median of each group. (**L**) Left: Integrated GFP intensity of GFP$^+$ PC3 cancer cells across 60 hours with the indicated engineered T cell treatment (E:T = 0.5:1). Right: Integrated GFP intensity of GFP$^+$ PC3 cancer cells treated with mock or CD5 KO CART–HER2 at the 60-hour time point. (**M**) Left: Integrated GFP intensity of GFP$^+$ DM6 cancer cells across 60 hours with the indicated engineered T cell treatment (E:T= 5:1). Right: Integrated GFP intensity of GFP$^+$ DM6 cancer cells treated with TRAC or TRAC CD5 KO TCR-*GP100* at the 60-hour time point. Student's *t* test was used to compare two groups; in analyses where multiple groups were compared, one-way ANOVA was performed with Tukey correction. Survival curves were compared using the log-rank (Mantel-Cox) test. *$P < 0.05$, **$P < 0.01$, ***$P < 0.001$, and ****$P < 0.0001$. MOS, median overall survival; ns, not significant.

as measured by both tumor volume and the more sensitive bioluminescence (Fig. 3, E and F). Similarly to the previously studied liquid cancer models, there was a numerical increase in the number of T cells in the peripheral blood of mice treated with CD5 KO CARTmeso cells (Fig. 3G). In the primary failure model, which included low CAR T doses, CD5 KO CARTmeso cells again demonstrated enhanced tumor control and longer overall survival compared with mock KO CARTmeso cells (median overall survival for mock KO CARTmeso = 46 days versus CD5 KO CARTmeso = 102 days; $P = 0.14$, Mantel-Cox; Fig. 3, H and I). This enhanced survival was again associated with increased T cell expansion and persistence (Fig. 3J). Last, to assess whether CD5 KO CARTmeso cells can establish prolonged immune memory, long-term surviving mice were rechallenged with the same tumor (day 74, 2×10^6 AsPC1 cells). CD5 KO CARTmeso cells did not show tumor engraftment, whereas control mice did (Fig. 3K and fig. S4, C to E), suggesting that CARTmeso cells are able to establish immunological memory in these models.

To further confirm the activity of CD5 KO as a generalizable strategy to enhance CAR T immunotherapy for solid cancers, we tested an additional solid cancer model using mock KO or CD5 KO CART-HER2 (4D5 clone) cells (*28*) and the $HER2^{+\,(dim)}$ prostate cancer cell line PC3. CAR T cells and PC3 cells were cocultured for 60 hours, and the cytotoxicity of each CAR T product was measured using live imaging. CD5 KO CART–HER2 cells demonstrated higher tumor killing as compared with mock KO CART-HER2 cells (Fig. 3L). Last, we hypothesized that the strategy of knocking out CD5 could be translated into a wide range of immunotherapies in addition to CAR T treatment, such as engineered TCR therapy, to enhance their efficacy in the clinic. To this goal, we generated TCRα constant (TRAC) KO T cells (*29*) further transduced with TCR-*GP100* lentivirus (*30*) and compared these to cells with a double KO (DKO) of both TRAC and CD5 using the $GP100^+$ melanoma cell line DM6. TRAC CD5 KO TCR-*GP100* cells showed reduced $GP100^+$ DM6 tumor growth in vitro when compared with TRAC KO TCR-*GP100* cells using a live imaging system (Fig. 3M), confirming that CD5 KO could enhance the efficacy of adoptive T cell therapies as a whole.

CD5 deletion enhances CAR T cell activation and cytotoxic machinery

Given the high killing activity of CD5 KO CAR T cells both in vitro and in vivo, we aimed to define the mechanisms by which CD5 KO enhances CAR T cell antitumor efficacy. In the context of TCR activation, CD5 recruits several inhibitory mediators to the cell membrane, such as SHP1, CBL-B, CBL, and others (Fig. 4A) (*31*–*35*). These factors are known to negatively regulate T cell activation by diminishing the expression and activity of phospholipase C–γ (PLCγ), a key protein involved in activating transcription factors activating protein 1 and nuclear factor κB, as well as intracellular calcium release to activate transcription factor NFAT (*36*). We hypothesized that the deletion of CD5 might abrogate these mediators' functions, leading to increased downstream signaling. Bulk RNA sequencing analysis of mock KO and CD5 KO CART5 cells demonstrated strong differential gene expression between the two groups (Fig. 4B). Gene set enrichment analysis revealed several pathways related to the PLCγ pathway, such as calcium-dependent events and diacylglycerol (DAG)–inositol 1,4,5-trisphosphate (IP_3) signaling (Fig. 4C) to be enriched in CD5 KO CART5 cells. DAG is known to play a crucial role in activating the Ras/extracellular signal–regulated kinase (ERK) pathway in T cells (*37*, *38*). To further understand the role of CD5 KO in CAR T function, we used phospho-flow cytometry and measured phospho-ERK1/2 within the Ras/ERK signaling pathway and phospho-S6 for insights into the phosphatidylinositol 3-kinase/AKT/mTOR pathway. In experiments where CD5 KO CART19 cells were cocultured with $CD19^+$ Nalm6 cells, we observed an increase in the phosphorylation of these markers, indicating enhanced activation compared with mock KO CART19 cells (Fig. 4D). This observation aligns with prior findings that have shown a rise in ERK (*33*, *39*) and S6 phosphorylation (*40*) after CD5 inhibition or deletion. Collectively, these data further suggest that CD5 acts as an inhibitory molecule in T cells and that its KO could prime CAR T cells to be more prone to increased activation upon stimulation.

To better understand the differences between mock KO and CD5 KO CAR T cells in vivo, we conducted single-cell RNA sequencing on human CAR T cells harvested from a xenograft mouse model. Mice were first engrafted with $CD19^+$ diffuse large B cell lymphoma (DLBCL) OCI-Ly18 and subsequently treated with mock or CD5 KO CART19 T cells. The study was terminated at an early stage, on day 16 after CART infusion, and T cells from mice treated with either mock KO or CD5 KO CART19 cells were harvested and subjected to single-cell RNA sequencing (Fig. 4E). We identified several clusters of $CD4^+$ and $CD8^+$ T cells with different memory subsets (Fig. 4F). We focused on cluster 7 because it was enriched in CD5 KO CART19 cells (fig. S5A). This group was identified to be a $CD8^+$ cluster that showed profound enrichment of key genes representative of tumor-reactive, cytotoxic T cells such as *PRF1*, *GZMB*, *CCL3*, *CCL4*, *IFNG*, *NKG7*, and *CST7* (Fig. 4G and fig. S5, B and C) (*41*–*43*). Gene set enrichment analysis of gene ontology on cluster 7 indicated that pathways related to cell killing and cytotoxicity are predominantly enriched in CD5 KO CART19 cells (Fig. 4G). These results were confirmed when comparing the entirety of CD5 KO CART19 cells with mock KO CART19 cells across all clusters, strongly suggesting that CD5 KO enhances the effector functions of $CD4^+$ and $CD8^+$ CAR T (Fig. 4H and fig. S5D). To confirm the RNA expression data with protein analyses, we conducted cytokine profiling of mouse serum 7 to 10 days after infusion with either mock KO or CD5 KO CART19 cells in a B-ALL model. In this analysis, we noted elevated concentrations of the corresponding proteins of several genes that were previously observed to be up-regulated in the single-cell RNA sequencing data, including *CCL3* (MIP-1α), *CCL4* (MIP-1β), and *IFNG* (interferon-γ; fig. S5E).

CD5 is able to recruit SHP1 (*PTPN6*) to the synapse. SHP1 is a phosphatase that dampens TCR signaling by dephosphorylating multiple targets. Given the connection between CD5 and the recruitment of SHP1, we sought to compare the functionality of CD5 KO CAR T cells with that of SHP1 KO CAR T cells (fig. S5F) and whether SHP1 KO could enhance CD5 KO. CD5 KO CAR T cells exhibited superior tumor control and overall survival compared with SHP1 KO cells (Fig. 4, I and J). Furthermore, when both SHP1 and CD5 were knocked out simultaneously, the tumor suppression and survival were equally effective as those achieved by CD5 KO CAR T cells.

Moreover, we sought to exclude whether the increased activity of CD5 KO CAR T cells in our xenograft models was, in part, because of TCR stimulation in the setting of a xenograft model [xenogeneic graft-versus-host disease (GVHD)]. To this goal, we used mice lacking WT major histocompatibility complex (MHC) I/II (*44*) that do not trigger xenogeneic GVHD because of lack of interaction with

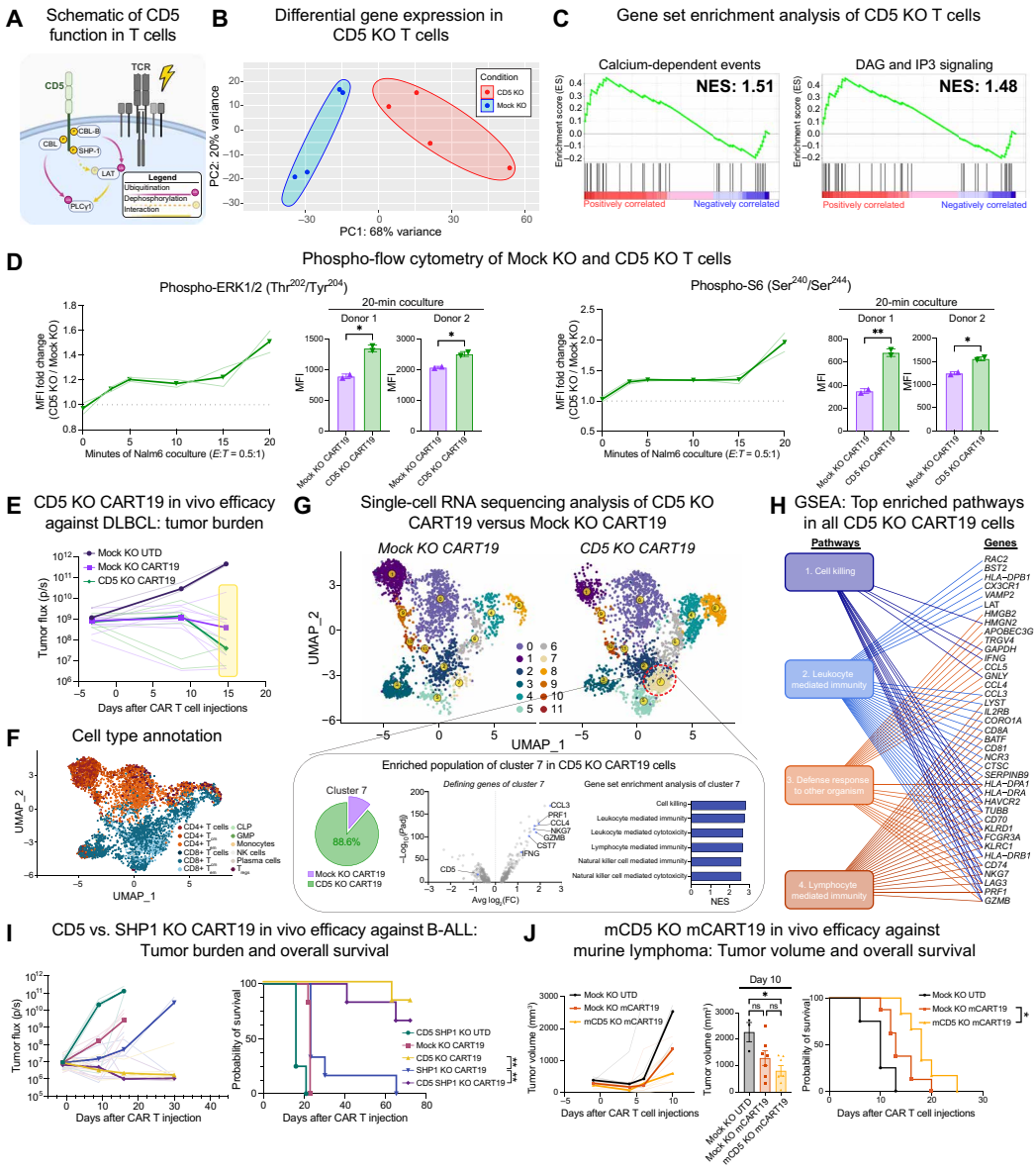

Fig. 4. CD5 deletion enhances CAR signaling. (**A**) Schematic describing the inhibitory role of CD5 in T cell activation: Upon activation, CD5 recruits several mediators to the cell membrane, including SHP1, CBL, and CBL-B. CBL ubiquitinates and promotes the degradation of PLCγ1, reducing total protein levels. SHP1 dephosphorylates LAT, an upstream positive regulator of PLCγ1, whereas CBL-B ubiquitinates and promotes its degradation. (**B**) Principal components analysis shows distinct grouping of mock KO and CD5 KO CART5 cells. $n = 2$ donors. (**C**) Gene set enrichment analysis identifies calcium-dependent events and DAG and IP_3 signaling as enriched pathways within CD5 KO CART5 cells. NES, normalized enrichment score. (**D**) For each indicated marker, (left) fold change of CD5 KO CART19 MFI/mock KO CART19 MFI of phosphorylated marker at indicated time points. (Right) MFI values of phosphorylated marker in mock KO CART19 and CD5 KO CART19 cells in two separate donors. (**E**) NSG mice were engrafted with 5×10^6 OCI-Ly18 DLBCL cells (subcutaneously) on day −10 and injected with 4×10^6 mock or CD5 KO CART19 cells (intravenously) on day 0. Bioluminescence imaging of tumor burden in each NSG mouse ($n = 3$ to 8 mice per group) engrafted with OCI-Ly18 cell line. The bolded line represents the median of each group. (**F**) Cell type annotations defined by colors indicating different cell types in the dataset. (**G**) Top: Uniform manifold approximation and projection (UMAP) of all clusters among mock KO CART19 and CD5 KO CART19 populations. Bottom: Volcano plot of differentially expressed genes in cluster 7 compared with all other clusters and gene set enrichment analysis of top pathways enriched in cluster 7. (**H**) Top enriched pathways defined by gene set enrichment analysis of all CD5 KO CART19 cells and the associated genes. (**I**) NSG mice were engrafted with 1×10^6 Nalm6 B-ALL cells (intravenously) on day −6 and injected with 0.75×10^6 mock or CD5 KO or SHP1 KO CART19 cells (intravenously) on day 0. Left: Bioluminescence imaging of tumor burden in each NSG mouse ($n = 4$ to 6 mice per group) engrafted with Nalm6 B-ALL cell line. The bolded line represents the median of each group. Right: The survival rate of each treatment group in xenograft B-ALL model is shown in a Kaplan-Meier survival curve [compared using log-rank (Mantel-Cox) test]. (**J**) NSG mice were engrafted with 2×10^6 A20 BCL cells (subcutaneously) on day −22, injected with cyclophosphamide (100 mg/kg, intraperitoneally) on day −1, and injected with 0.3×10^6 mock or mCD5 KO mCART19 cells (intravenously) on day 0. Left: Tumor volume (in mm^3) in each BALB/c mouse ($n = 4$ to 7 mice per group) engrafted with A20 murine lymphoma cell line. The bolded line represents the median of each group. Middle: Tumor volume (in mm^3) in each BALB/c mouse engrafted with A20 murine lymphoma on day 10 after CAR T cell injections. Right: The survival rate of each treatment group in xenograft A20 model is shown in a Kaplan-Meier survival curve (compared using the Gehan-Breslow-Wilcoxon test). Student's *t* test was used to compare two groups; one-way ANOVA was performed with Tukey correction for multiple comparisons. $^*P < 0.05$, $^{**}P < 0.01$, $^{***}P < 0.001$, and $^{****}P < 0.0001$.

the TCR (fig. S5G). In this model, we compared mock KO and CD5 KO CARTmeso cells against mesothelin$^+$ AsPC1. Although these mice lacked MHC I/II, CD5 KO CARTmeso cells expanded and controlled tumor growth as compared with mock KO CARTmeso cells (fig. S5G), confirming that the expansion is specific to CAR activation and not confounding TCR activation.

CD5 KO T cells display heightened functions in vivo in an immunocompetent cancer model

The xenograft cancer models used thus far lacked a functional immune system and the immunosuppressive tumor microenvironment (TME), which may not entirely mirror what is observed in patients. To assess whether CD5 KO could enhance the efficacy of adoptive cell therapies in a setting where the immune system operates fully, we established an immunocompetent CAR T model using murine CART19 and the A20 B-cell lymphoma model (*45*). We first developed a strategy to perform CRISPR-Cas9 in murine CAR T cells. Briefly, a sgRNA against murine CD5 (mCD5) was designed and used to knock out mCD5 in primary BALB/c murine T cells (fig. S5H and table S2). We then used a murine gammaretroviral particle to transduce a CAR construct targeting murine CD19 (fig. S5H). We tested these mCD5 KO T cells targeting murine CD19 (mCD5 KO mCART19) against the mCD19$^+$ lymphoma cell line A20 in BALB/c mice. In this model, mice were injected with A20 cells and treated with a low dose of CAR T cells or an equal number of control UTD cells after lymphodepletion with cyclophosphamide (100 mg/kg). At the time of infusion, A20 tumors measured an average of ~300 mm^3. Although only around 50% of the mCART19 cells showed successful KO of mCD5 in the mCD5 KO mCART19 group (fig. S5H), this group nonetheless slowed down tumor growth and significantly extended overall survival when compared with control mock KO CART19 cells (median overall survival for mock KO mCART19 = 13 days versus mCD5 KO mCART19 = 18 days; $P = 0.0321$, Gehan-Breslow-Wilcoxon; Fig. 4K). These results suggest that signaling pathways downstream of mCD5 suppress T cell–mediated tumor control in a fully preserved TME.

Superior tumor control is demonstrated by CD5 KO as compared with PD-1 deletion in liquid and solid cancer models

PD-1 is a critical immune checkpoint in T cells, and several immune checkpoint inhibitors targeting the PD-1:ligand 1 (PD-L1) axis are routinely used in the clinic (*46*). More recently, checkpoint inhibition has been shown to enhance CAR T immunotherapy in subsets of patients (*47*). Furthermore, deletion of PD-1 in adoptively transferred T cells has been described as a possible strategy to reduce T cell exhaustion, thereby enhancing the antitumor activity. A pivotal report demonstrated the feasibility of this approach for patients with myeloma or sarcoma using PD-1 KO in engineered TCR T cells (*48*). Since then, many clinical trials are currently testing PD-1 KO or inhibition in CAR T therapy for cancer (NCT04539444, NCT03298828, NCT04381741, NCT03287817, NCT03030001, NCT03182803, and NCT03545815), indicating PD-1 as an ideal comparator to assess the relative efficacy of CD5 KO in enhancing CAR T therapy.

We aimed to compare this established strategy to reduce T cell exhaustion with the disinhibition of early CAR T activation by CD5 deletion. We used the clinically relevant sgRNA (*48*) to knock out PD-1 from CART19 cells (fig. S6A and table S2). We first compared CD5 KO to PD-1 KO CART19 against the standard CD19$^+$ B-ALL cell line Nalm6. In a high CAR T dose model (1×10^6 CAR$^+$ T cells), both CD5 and PD-1 KO enhanced CAR efficacy equally as compared with mock KO CART19 cells (fig. S6, B and C). However, when we tested these cells in a "stress" model, with lower CAR T doses (0.35×10^6 CAR$^+$ T cells), PD-1 KO CART19 were unable to enhance CAR T efficacy, whereas CD5 KO CART19 cells maintained strong tumor control (Fig. 5A). This enhanced tumor control also correlated with increased overall survival (Fig. 5B) (median overall survival for mock KO CART19 = 20 days versus PD-1 KO CART19 = 26 days versus CD5 KO CART19 = undefined) and increased T cell count in the peripheral blood on day 14 (Fig. 5C).

We then compared CD5 KO versus PD-1 KO in a solid tumor model of PDAC. We compared CD5 KO with PD-1 KO CARTmeso against the mesothelin$^+$ PDAC cell line AsPC1 in NSG-MHC I/II double KO (DKO) mice (fig. S6, D and E). CD5 KO CARTmeso cells demonstrated enhanced tumor control and stronger response rates as determined by tumor volume and bioluminescence imaging (Fig. 5, D and E). This increased tumor control allowed for enhanced survival (median overall survival Mock KO CARTmeso = 71 days versus PD-1 KO CARTmeso = 85 days versus CD5 KO CARTmeso = undefined; Fig. 5F). Furthermore, we observed a significantly increased T cell count in CD5 KO CARTmeso–treated mice as compared with controls (Fig. 5G).

Evaluation of the safety of CD5 KO reveals limited toxic effects

Any gene editing approach carries the risk of off-target unwanted mutations. To verify the accuracy of our CD5 KO approach, we performed iGUIDE-sequencing (improved genome-wide, unbiased identifications of double-stranded breaks enabled by sequencing) (*49*, *50*). In this study, we confirmed high on-targeted cleavage with no off-target cleavage sites of concern detected when using this sequence within two separate donors (fig. S7A). The top five off-target genes by TrueCut Cas9 or SpyFi Cas9 include *CALCP*, *C20orf85*, *INPP4B*, *XPO7*, and *SLC10A7*. All five potential genes demonstrate little to no expression in CD4$^+$ or CD8$^+$ naïve T cells as seen by bulk RNA sequencing analysis data (https://dice-database.org; fig. S7B), indicating no obvious basis for concern regarding the location of off-target cleavage sites.

Another potential issue with an approach that strongly enhances CAR T activity is the possibility of on-target CAR T transformation or non–antigen-specific reactivity. To evaluate these risks and the potential toxicities of CD5 KO in T cells, we performed cytokine-independent CAR T proliferation assays and in vivo toxicity xenograft models. CD5 KO UTD or CAR T cells did not grow aberrantly without growth/survival-associated cytokines [interleukin-2 (IL-2)/IL-7/IL-15], suggesting that these cells still depend on cytokine or antigen stimulation (fig. S7C). We further evaluated the potential tumorigenicity of CD5 KO CAR T cells by evaluating their ability to form colonies using a soft agar colony formation assay. When 5000 or 10,000 cells per agarose gel were seeded, only Jurkat cells (positive control) were able to form colonies, whereas CD5 KO CART5 cells did not grow (fig. S7D).

We then evaluated whether CD5 KO CAR T cells would generate nonspecific tissue damage in NSG mice (xenogeneic recognition). To this goal, we compared CD5 KO CAR T5 with UTD T cells or the gold standard CART19 product in vivo in NSG mice engrafted with green fluorescent protein–positive (GFP$^+$) Jurkat cells. Although this model is

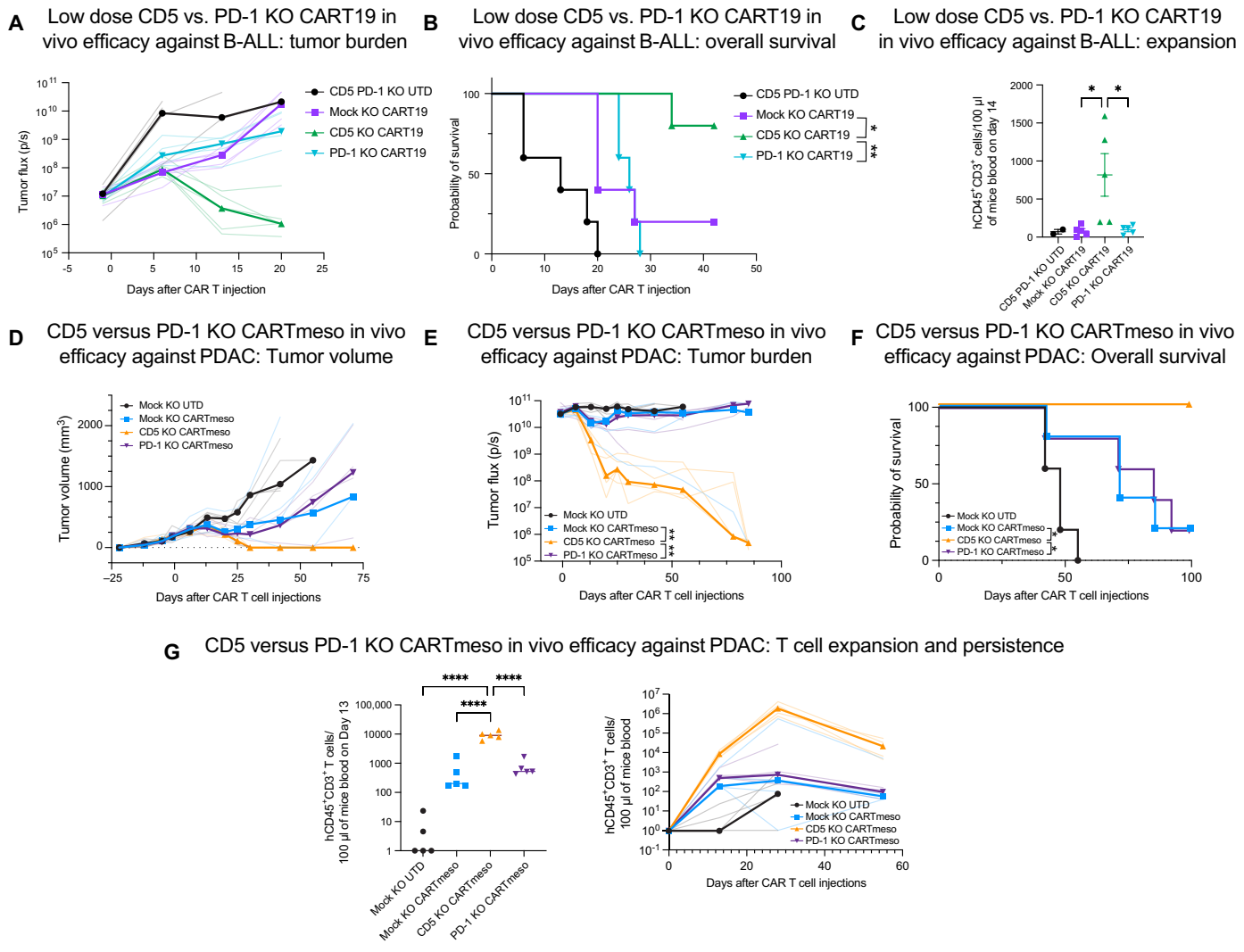

Fig. 5. Comparison of CD5 KO with PD-1 KO in CAR T therapy. (**A**) NSG mice were engrafted with 1×10^6 Nalm6 B-ALL cells (intravenously) on day −6 and injected with 0.35×10^6 mock or CD5 KO or PD-1 KO CART19 cells (intravenously) on day 0. Bioluminescence imaging of tumor burden in each NSG mouse ($n = 5$ mice per group) engrafted with Nalm6 B-ALL cell line. The bolded line represents the median of each group. (**B**) The survival rate of each treatment group in xenograft B-ALL model is shown in a Kaplan-Meier survival curve. (**C**) Absolute cell counts of $hCD45^+hCD3^+$ T cells in 100 µl of mouse blood at day 14. (**D**) NSG MHC I/II DKO mice were engrafted with 2×10^6 AsPC1 PDAC cells (subcutaneously) on day −27 and injected with 0.5×10^6 mock or CD5 KO or PD-1 KO CARTmeso cells (intravenously) on day 0. Tumor volume (in mm^3) in each NSG-MHC I/II DKO mouse ($n = 5$ mice per group) engrafted with AsPC1 PDAC cell line. The bolded line represents the median of each group. (**E**) Bioluminescence imaging of tumor burden in each NSG-MHC I/II DKO mouse. The bolded line represents the median of each group. (**F**) The survival rate of each treatment group in xenograft PDAC model is shown in a Kaplan-Meier survival curve. (**G**) Left: Absolute cell counts of $hCD45^+hCD3^+$ T cells in 100 µl of mouse blood at day 13. Right: Absolute cell counts of $hCD45^+hCD3^+$ T cells in 100 µl of mouse blood over time. The bolded line represents the median of each group. One-way ANOVA was performed with Tukey correction for multiple comparisons; survival curves were compared using the log-rank (Mantel-Cox) test. $^*P < 0.05$, $^{**}P < 0.01$, $^{***}P < 0.001$, and $^{****}P < 0.0001$.

constrained by its lack of human CD5 expression, it was specifically designed to evaluate potential nonspecific tissue damage that could arise from cytokine release, inflammation, or nonspecific TCR/MHC interactions, also known as xenogeneic GVHD. This test is mandated by the FDA as a standard for toxicity assessment. On day 10 after CAR T injections, animals were euthanized, and a complete necropsy was performed on all animals (figs. S8 and S9). We analyzed different tissues using microscopy after hematoxylin and eosin staining and GFP staining for cancer cell detection. No treatment-related tissue lesions were observed in CD5 KO CART5 cells as compared to controls (fig. S8), and GFP^+ tumor cells were present in controls but not in CD5 KO CART5 mice. Moreover, mice were monitored for clinical signs and weight. Although mice treated with UTD T cells or CART19 demonstrated overall and organ-specific weight loss because of tumor progression, CD5 KO CART5 mice showed progressively increasing weight, another sign of lack of apparent toxicities such as tissue damage or cytokine-release syndrome (fig. S9A). Last, blood and serum analyses such as complete blood counts and biochemistry were performed, and we found no differences in their clinical chemistry profile or complete blood counts (fig. S9, B and C).

Strong clinical relevance seen between CD5 expression in T cells and cancer outcomes

To confirm the clinical relevance of the inhibitory role of CD5 in cancer, we retrospectively investigated whether the expression of *CD5* relative to *CD3ε* (to normalize for T cell infiltration) in biopsies of patients with cancer correlated with overall survival (*51*). We analyzed The Cancer Genome Atlas database, which contains the RNA sequencing data on more than 9000 biopsies of more than 33 human cancer types. In the entire cohort, low *CD5/CD3ε* expression in pretreatment biopsies correlated with significantly improved overall survival ($P = 0.0017$; fig. S10A). A similar outcome was observed when analyzing data for the checkpoint receptor *PCDC1* (PD-1), whose inhibition with antibodies such as nivolumab or pembrolizumab has led to long-term complete responses in relapsed or refractory cancers (fig. S10A) (*46*). We then focused on a highly immunogenic cancer, skin cutaneous melanoma, and observed a strong correlation between low *CD5/CD3ε* expression and survival ($P = 0.0023$; fig. S10B). Overall, looking at all the different cancer types, low *CD5/CD3ε* expression correlated with better survival in 12 of 33 cancers, whereas low *PCDC1/CD3ε* correlated in 10 of 33.

Last, to directly evaluate the potential efficacy of CD5 in the context of CAR T immunotherapies within clinical settings, we conducted an analysis encompassing both 4-1BB– and CD28-costimulated CART19 treatments, namely, axicabtagene ciloleucel (axi-cel) and tisagenlecleucel (tisa-cel). Our initial investigation focused on the baseline tisa-cel product obtained from 13 patients diagnosed with NHL using the single-cell RNA sequencing dataset sourced from the work of Haradhvala *et al.* (*52*) (Gene Expression Omnibus accession number GSE197268). Nonresponder patients exhibited notably elevated *CD5* RNA expression compared with complete responder patients ($P < 0.0001$; Fig. 6A and fig. S10C). Our findings indicated that on day 7 after axi-cel treatment, complete responder patients displayed substantially lower amounts of *CD5* RNA expression in peripheral blood cells compared with nonresponders ($P < 0.0001$; Fig. 6B and fig. S10C). Collectively, these results imply a correlation between diminished CD5 expression and enhanced antitumor effects of CART19 products within clinical contexts, thereby reinforcing the pivotal role of CD5 in the functionality of CAR T cells.

Clinical development of a 5-day manufactured CD5 KO CART5 product for a phase 1 clinical trial for nonleukemic CD5$^+$ TCLs

On the basis of the promising results described above, we sought to translate CD5-deleted anti-CD5 CAR T to the clinic for the treatment of patients with CD5$^+$ TCL. To this end, we modified the manufacturing protocol, shortening it from ~15 to 5 days (Fig. 7A). Because the SpyFi Cas9 protein demonstrated lower off-target effects in iGUIDE-sequencing experiments as compared with TrueCut Cas9 (fig. S7A), we optimized our protocol to use SpyFi Cas9. We used the MaxCyte electroporation platform given the extensive clinical use and experience with that system (*48*). We also revised the T cell activation strategy and adopted the biodegradable CD3/CD28 stimulation reagent (TransAct) in place of magnetic CD3/CD28 Dynabeads with the goal of decreasing cell loss from debeading. The rapid manufacturing protocol was optimized such that cells were electroporated and activated both on day 0, rather than on days 0 and 1, as in the conventional manufacturing. Consequently, lentiviral transduction was performed on day 1 instead of day 2. With this protocol, we observed CAR expression and CD5 KO peaking 1 day sooner in cells produced by rapid manufacturing (CD5 KO CART5$_{rapid}$) as compared with cells generated by the conventional manufacturing protocol (CD5 KO CART5$_{conv}$) without compromising population doublings (Fig. 7B). At the end of expansion, CD5 KO CART5$_{rapid}$ cells demonstrated a more activated, central memory–like phenotype as compared with CD5 KO CART5$_{conv}$ manufactured cells (Fig. 7C). Furthermore, at baseline, CD5 KO CART5$_{rapid}$ cells exhibit elevated expression of degranulation and cytokine release compared with CD5 KO CART5$_{conv}$ cells. However, upon activation through coculture with CD5$^+$ Jurkat cells, the expression in both groups shows relatively similar responses (Fig. 7D).

To compare the efficacy of CD5 KO CART5 generated using both protocols, we performed an in vitro experiment against CD5$^+$ Jurkat. At a reduced E:T ratio of 0.0625:1, CD5 KO CART5$_{rapid}$ cells exhibited enhanced cytotoxic effectiveness against Jurkat cells relative to CD5 KO CART5$_{conv}$ cells. As expected, with increased E:T ratios, the tumors were completely eradicated, thereby preventing the possibility to detect any noticeable differences between the two groups (Fig. 7E). This was further supported by in vivo evidence, where mice treated with CD5 KO CART5$_{rapid}$ cells demonstrated stronger antitumor responses compared with CD5 KO CART5$_{conv}$ (Fig. 7F), likely because of its more activated state at the time of injection. This increased tumor control correlated with increased overall survival of mice treated with CD5 KO CART5$_{rapid}$ (median overall survival CD5 KO CART5$_{conv}$ = 44 days versus CD5 KO CART5$_{rapid}$ = undefined; $P = 0.0019$, Mantel-Cox; Fig. 7G) and higher expansion of CD5 KO CART5$_{rapid}$ cells in the peripheral blood (Fig. 7H).

In conclusion, this study demonstrates that CD5 is a negative regulator and potential immune checkpoint for adoptive T cell immunotherapies. We show that CD5 deletion leads to the enhancement of CAR–T cell function in vivo in several clinically relevant models of liquid and solid tumors. This effect is mediated by an enhanced effector

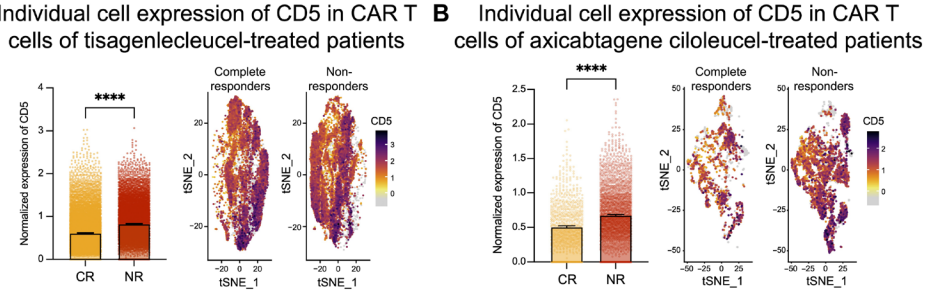

Fig. 6. Real-world survival data of CD5 expression in T cells. (**A**) *CD5* expression in CAR T cell infusion products of patients treated with the FDA-approved CART19 product tisagenlecleucel [complete responders (CR): $n = 5$ patients, 29,811 total cells; nonresponders (NR): $n = 8$ patients, 30,949 total cells]. (**B**) *CD5* expression in CAR T cells on day 7 of patients treated with the FDA-approved CART19 product axicabtagene ciloleucel (CR: $n = 5$ patients, 2727 total cells; NR: $n = 6$ patients, 6374 total cells). Student's *t* test was used to compare two groups. ****$P < 0.0001$.

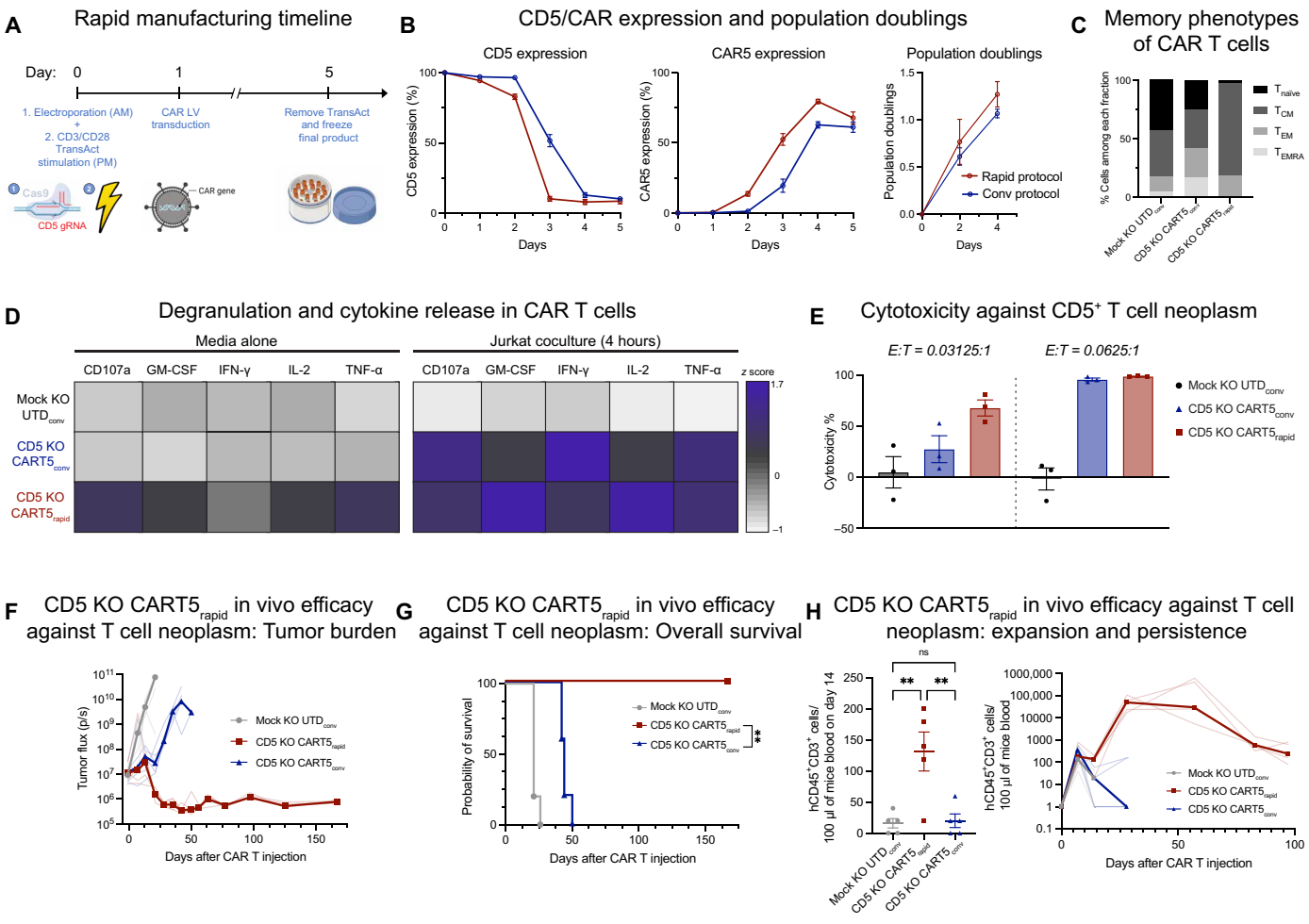

Fig. 7. Development of a clinical-grade, rapidly manufactured CD5 KO CART5 product. (**A**) Rapid CD5 KO CAR T manufacturing protocol. T cells are electroporated and stimulated both on day 0 and transduced with CAR lentivirus on day 1, and the final product is frozen on day 5. (**B**) CD5 expression, CAR5 expression, and population doublings were monitored and recorded for 4 to 5 days in CD5 KO CART5 cells manufactured by either the rapid-manufacturing or the conventional-manufacturing protocol. (**C**) T cell memory phenotypes of each engineered T cell group after thaw. (**D**) Heat map of *z* score normalized levels of CD107a, granulocyte-macrophage colony-stimulating factor (GM-CSF), IFN-γ, IL-2, and tumor necrosis factor–α in CD5 KO $CART5_{rapid}$ and CD5 KO $CART5_{conv}$ T cells, with and without 4-hour activation by coculture with Jurkat (E:T = 1:1). (**E**) Percent cytotoxicity of UTD or CART5 cells against $CD5^+$ Jurkat T-ALL cells after 72 hours. (**F**) NSG mice were engrafted with 1×10^6 Jurkat T-ALL cells (intravenously) on day −7 and injected with 0.5×10^6 CD5 KO $CART5_{rapid}$ or CD5 KO $CART5_{conv}$ cells (intravenously) on day 0. Bioluminescence imaging of tumor burden in each NSG mouse ($n = 5$ mice per group) engrafted with Jurkat T-ALL cell line. The bolded line represents the median of each group. (**G**) The survival rate of each treatment group in xenograft T-ALL model is shown in a Kaplan-Meier survival curve. (**H**) Left: Absolute cell counts of $hCD45^+hCD3^+$ T cells in 100 µl of mouse blood on day 14. Right: Absolute cell counts of $hCD45^+hCD3^+$ T cells in 100 µl of mouse blood over time. The bolded line represents the median of each group. One-way ANOVA was performed with Tukey correction for multiple comparisons; survival curves were compared using the log-rank (Mantel-Cox) test. $^{**}P < 0.01$.

and cytotoxic phenotype and increased expansion and persistence of the CD5 KO CAR T cells. In clinical samples, low *CD5* expression in tumor biopsies was associated with better survival, and CAR T cells from responding patients had lower *CD5* expression as compared with nonresponders. We have now defined an improved, rapidly manufactured protocol that will be used to test CD5 KO CAR T cells in a phase 1 clinical trial for $CD5^+$ relapsed and refractory TCL (NCT06420089).

DISCUSSION

The vast majority of patients treated with adoptive T cell therapies will eventually fail treatment. Therefore, there is a dire need to improve adoptive T cell immunotherapies to increase long-term responses. Furthermore, current CAR T products only target B cell malignancies and multiple myeloma, and existing research aims to expand their use for other cancers such as T cell malignancies.

In this study, we initially sought to develop CAR T for TCLs. Most CAR T cells designed for use against T cell malignancies focus on universal T cell markers like CD7 or CD5 (*53*, *54*). However, a considerable hurdle with these targets is the occurrence of fratricide, where T cells eliminate other T cells that express the target antigen, either during manufacturing or after infusion. Previous studies on CART5 cells have indicated minimal fratricide during manufacturing, but our results suggest that CD5:CAR5 recognition in our system leads to some degree of fratricide and CD5 down-regulation. This is in line with previous evidence that CD5 WT CD28ζ-based CART5 cells can be expanded in vitro (*55*) but is in

contrast with another report demonstrating the full fratricide of CD5 WT 4-1BB–based CART5 cells (*56*). This discrepancy is likely attributable to the distinct single-chain variable fragments used in those studies compared with this one and the fact that our approach uses a lentiviral platform in comparison with a retroviral one. One strategy used to overcome the fratricide issues associated with CART5 involves modifying the CART5 manufacturing by including the small-molecule inhibitors dasatinib and ibrutinib to reduce T cell activation likely caused by fratricide (*57*); however, further research is needed to assess the long-term clinical effectiveness of such a system. Our method leverages the clinically established CRISPR-Cas9 to completely abrogate CD5 from T cells, thereby eliminating the risk of fratricide during manufacturing and after infusion. In line with our findings, other groups have shown that CD5 deletion avoids fratricide in CART5 by using CRISPR-Cas9 (*22*) or base editing (*58*).

The critical novelty of this work relies on the finding that CD5 deletion enhances CAR T function in vivo in both liquid and solid cancer models by enhancement of T signaling, cytotoxicity, and persistence. The absence of CD5 strengthens CAR and TCR signaling, enhancing calcium-dependent events and DAG and IP_3 signaling, as seen by bulk RNA sequencing analysis and confirmed by phosphoflow cytometry. Mechanistically, we observed enrichment of highly cytotoxic CAR T in the CD5 KO group in vivo, as demonstrated by single-cell RNA sequencing. As a result, T cells with deleted CD5 exhibit augmented in vivo expansion and persistence in all tested models. Crucially, to assess whether CD5 KO outperforms the currently pursued KO strategies in clinical settings, we conducted a comparative analysis between CD5 KO and PD-1 KO. We chose PD-1 because of the extensive literature supporting the benefits of its blockade and the reported clinical outcomes of PD-1 KO using CRISPR-Cas9. We purposely selected a cell line (AsPC1) that expresses PD-L1, the ligand of PD-1, and one (Nalm6) that does not (*59*) to comprehensively assess the effect of the different gene edits. Our results demonstrated that CD5 KO outperformed PD-1 KO in both liquid and solid cancer models. This effect was linked to improved CAR T expansion and the sustained presence of CD5 KO, potentially aligning with recent findings suggesting that PD-1 KO might affect memory establishment (*60*). Numerous other KOs have been explored in preclinical models as strategies to enhance CAR T function, including *RASA2* (*61*), *PTPN2* (*62*), *TET2* (*63*), *CTLA4* (*59*), and several others. Although a comprehensive comparison with all of these KOs would be intriguing, we deemed it beyond the scope of this study and prioritized PD-1 as the single most relevant clinical target. The critical role of CD5 KO is bolstered by its validation in a total of seven cancer models, encompassing both liquid and solid tumors and using immunodeficient and immunocompetent mice. Furthermore, our findings held true when applied to TCR-redirected T cells, underscoring the generalized relevance of this pathway.

The current study also has limitations. First, any strategy aimed at enhancing CAR T functionality might lead to increased side effects in clinical settings, such as cytokine release syndrome/neurotoxicity due to enhanced CAR T proliferation and activation or autoimmunity due to TCR disinhibition. Although preclinical models are not always reliable for predicting human toxicities, we conducted Investigational New Drug application–standard studies to evaluate the potential adverse effects of CD5 KO. The enhanced functionality of CD5 KO CAR T was not linked to unregulated proliferation or cytokine-independent survival. We also carried out a mouse necropsy in a xenograft model of T cell leukemia and identified no tissue toxicity. Although this model does not replicate human CD5 expression, it was specifically designed to check for possible nonspecific tissue damage from factors like cytokine release, inflammation, or unrelated TCR/MHC interactions (xenogeneic GVHD). For this study, we used the most common method to inactivate protein expression in adoptive T cell therapy, which is CRISPR-Cas9 (*64*, *65*). Although the CRISPR platform has proven to be effective in patients and it is certainly the most clinically advanced one, there are still concerns/limitations, such as the potential off-target effects and chromosomal rearrangements that may occur during the process of double-stranded break repair (*48*, *64*, *66*, *67*). Although our initial decision to apply CRISPR-Cas9 technology to T cells before their activation was to minimize the coexpression of endogenous CD5 and the engineered CAR5 on the cell surface, recent studies have provided support for this specific sequencing, demonstrating it also to be beneficial for preventing chromosome loss in T cells (*68*). Furthermore, we did not find off-targets for the CD5 KO gRNA, but to avoid risks, it could be possible to develop antibody-mediated degradation of CD5. For example, previous studies have demonstrated that, upon binding, anti-CD5 monoclonal antibodies can trigger the internalization of the CD5:antibody complex (*39*, *69*–*71*), potentially mimicking CD5 KO. Our future studies will test and compare the efficacy of the two methods.

In summary, this research provides evidence that CD5 acts as an inhibitory regulator and could serve as a new immune checkpoint for adoptive T cell immunotherapy. We demonstrated that the elimination of CD5 boosts the functionality of CAR and TCR T cells in various clinically relevant models of liquid and solid tumors. These findings suggest that CD5 plays a pivotal role as a suppressor of T cell function and holds promise as a viable clinical target for bolstering T cell therapies. Encouraged by these promising findings, we are initiating a phase I clinical trial of the CD5 KO CART5 product for the treatment of $CD5^+$ relapsed and refractory TCL (NCT06420089).

MATERIALS AND METHODS

Study design

The primary aim of this study was to assess the impact of CD5 deletion in adoptive T cell therapies targeting various malignancies. We established an efficient CRISPR-Cas9–based protocol for CD5 KO in T cell therapies directed against diverse tumor antigens, including CD19 and mesothelin. To maintain statistical rigor, we conducted all in vivo experiments with a minimum number of mice per group ($n = 4$ to 8 mice per group), ensuring the reproducibility of observed statistical differences. We used randomization to ensure that the baseline tumor burden did not differ significantly among treatment groups, and treatments were administered in a blinded manner. All T cells used in this study were sourced from healthy volunteers through the Human Immunology Core (Institutional Review Board protocol number: 705906) at the Perelman School of Medicine, University of Pennsylvania. The University of Pennsylvania Institutional Animal Care and Use Committee granted approval for all animal experiments, and we conducted all animal procedures in accordance with both federal and Institutional Animal Care and Use Committee guidelines within the University of Pennsylvania's animal facility. All experimental protocols were subject to approval by

the Institutional Animal Care and Use Committee at the University of Pennsylvania.

Cell lines and primary samples

Unless otherwise specified, all cell lines were cultured in R10 media [RPMI 1640 (Gibco; catalog no.11875-085) supplemented with 10% fetal bovine serum (Gibco; catalog no. 16140-071), 1% penicillin and 1% streptomycin (Gibco; catalog no. 15140-163), 1% GlutaMAX supplement (Gibco; catalog no. 35050-079, and 1% Hepes (Gibco; catalog no. 15630-130)] in a 37°C incubator with 5% CO_2. All cell lines were authenticated by short tandem repeat analysis and tested for mycoplasma using a MycoAlert Plus Mycoplasma Detection Kit (Lonza; catalog no. LT07-710). Nalm6, Jurkat, human embryonic kidney (HEK) 293T, AsPC1, HDLM2, PC3, and OCI-Ly18 cell lines were purchased from the American Type Culture Collection or DSMZ. TH20, a primary PDX model of T-ALL, was gifted by D. Teachey. DM6 was gifted by B. Carreno. All cell lines were transduced with a lentivirus encoding click beetle green and GFP. When necessary, cell lines were sorted on a FACSMelody (BD) sorter machine to achieve >95% target cell population abundance. Primary T-ALL and primary Sézary cells for in vitro cytotoxicity assay were provided by the clinical practices of A. Rook. Platinum-E cells used for retrovirus production were cultured in D10 media (Dulbecco's modified Eagle's medium) supplemented with 10% fetal bovine serum, 1% penicillin and 1% streptomycin, and 1% GlutaMAX. A20 cells were cultured in R10 media supplemented with 0.05 mM 2-mercaptoethanol.

CD5 short gRNA optimization

CRISPR sgRNAs were designed using software integrated into Benchling (www.benchling.com). For each target gene, eight sgRNA sequences were designed to target early exon sequences (table S1) and in vitro transcribed using the GeneArt Precision gRNA Synthesis Kit (Invitrogen; catalog no. A29377) for screening. Cells were electroporated using the Lonza 4D-Nucleofector Core Unit. Primary T cells were electroporated using the P3 Primary Cell 4D-Nucleofector X Kit L (Lonza; catalog no. V4XP-3024). For Cas9 and sgRNA delivery, the ribonucleoprotein (RNP) complex was initially formed by incubating 10 μg of TrueCut Cas9 protein v2 (Lonza; catalog no. A36499) with 5 μg of sgRNA for 10 min at room temperature for every. Cells (10×10^6) were spun down at 300*g* for 5 min and resuspended in 100 μl in the specified buffer. The RNP complex and 100 μl of resuspended cells were combined and electroporated using pulse code EO-115. After electroporation, the cells were incubated in standard medium containing supplemental cytokines IL-7 and IL-15 (20 ng/ml) at a concentration of 2×10^6 cells/ml at 37°C. CD5 expression was subsequently monitored at each of the indicated days. After initial CD5 sgRNA screening (fig. S1C), all experiments were performed using CD5_gRNA_4.

Lentivirus production

Replication-defective, third-generation lentiviral vectors were produced using HEK293T cells. About 8×10^6 cells were plated in T150 culture vessels in standard culture media and incubated overnight at 37°C. Eighteen to 24 hours later, cells were transfected using a combination of Lipofectamine 2000 (116 μl; Invitrogen; catalog no.11668-019), pVSV/G or pCocal (7 μg), pRSV/Rev. (18 μg), pGag/Pol (18 μg) packaging plasmids, and 15 μg of expression plasmid [CART5, 17H2L (*23*); CART19, FMC63; CART30, TI-159 (*25*); CARTmeso, M5; CART-HER2, 4D5; and TCR-*GP100*, *TCR976* (*HLA-A*02:01/G280*)]. Lipofectamine and plasmid DNA were diluted in 4 ml of Opti-MEM media (Gibco; catalog no. 31985-070) before transfer into lentiviral production flasks. At both 24 and 48 hours after transfection, the culture medium was isolated and concentrated using high-speed ultracentrifugation (8500 rpm overnight or 25,000 rpm for 2.5 hours). All CAR constructs were composed of a single-chain variable fragment (scFV), 4-1BB costimulatory domain, and CD3ζ costimulatory domain, unless otherwise noted.

Retrovirus production

MuCAR19-MSGV (murine stem cell virus–based splice-gag vector) is a 4-1BB costimulated CD3z CAR construct targeting murine CD19 in an MSGV. About 8×10^6 cells were plated in T150 culture vessels in the D10 aforementioned culture medium and incubated overnight at 37°C. Eighteen to 24 hours later, cells were transfected using a combination of Lipofectamine 2000 (60 μl; Invitrogen; catalog no.11668-019) and muCAR19-MSGV retroviral construct (15 μg). Lipofectamine and plasmid DNA were diluted in 3 ml of Opti-MEM media (Gibco; catalog no. 31985-070) before transfer into retroviral production flasks. At both 48 and 72 hours after transfection, the culture medium was isolated, filtered (0.45 μm), combined to be flash-frozen, and stored in −80°C.

Manufacturing of primary human genome-engineered CAR T cells (conventional manufacturing)

Human T cells were procured through the University of Pennsylvania Human Immunology Core. $CD4^+$ and $CD8^+$ cells were combined at a 1:1 ratio and used for electroporation. CRISPR-Cas9 sgRNAs were either generated through in vitro transcription using the GeneArt Precision gRNA Synthesis Kit (Invitrogen; catalog no. A29377) or chemically synthesized (Integrated DNA Technologies or Synthego). CD5 sgRNA sequences are listed in table S1. All other sgRNA sequences used are listed in table S2. sgRNAs (5 μg) were premixed with 10 μg of TrueCut Cas9 protein v2 (Invitrogen; catalog no. A36499; or SpyFi Cas9 when noted; Aldevron; catalog no. 9214-5MG) for 10 min at room temperature to form an RNP complex before electroporation. T cells (10×10^6) in 100 μl of the buffer provided with P3 Primary Cell 4D-Nucleofector X Kit L (Lonza; catalog no. V4XP-3024) were mixed with the RNP complex and subsequently electroporated using the pulse code EO-115 in a 4D-Nucleofector (Lonza; catalog no. AAF-1002B). Mock KO cells were electroporated using the same procedure as described without the presence of an RNP complex. After electroporation, T cells were incubated at 37°C for 24 hours and subsequently activated using CD3/CD28 Dynabeads (Gibco; catalog no. 40203D) at a ratio of three beads per cell. The following day, CAR lentiviral vectors were added to stimulated cultures at a multiplicity of infection between 1 and 3. Beads were removed between days 6 and 8 of stimulation, and cells were counted every other day using a Multisizer 3 Coulter Counter (Beckman) or Moxi GO II (Orflo) until growth kinetics and cell size demonstrated that they had rested from stimulation. All T cells were initially grown with supplemental cytokines IL-7 and IL-15 (20 ng/ml) that was decreased to 0 ng/ml by the end of the expansion.

Statistical analysis

Data were visualized and analyzed using Prism 9 software (GraphPad). All results are represented as either individual values or as means ± SEM unless otherwise noted. All comparisons between two groups

were performed using two-tailed unpaired Student's *t* test. Comparisons between more than two groups were performed by one-way analysis of variance (ANOVA) with Tukey correction. In analyses where multiple groups were compared at multiple time points/ratios, two-way ANOVA was performed. Survival data were analyzed using the log-rank (Mantel-Cox) test unless otherwise noted. The *P* values were denoted with asterisks as follows: $*P < 0.05$, $**P < 0.01$, $***P < 0.001$, and $****P < 0.0001$.

Supplementary Materials

The PDF file includes:
Methods
Figs. S1 to S10
Tables S1 and S2

Other Supplementary Material for this manuscript includes the following:
Data files S1 and S2
MDAR Reproducibility Checklist

REFERENCES AND NOTES

1. M. Cerrano, M. Ruella, M. A. Perales, C. Vitale, D. G. Faraci, L. Giaccone, M. Coscia, M. Maloy, M. Sanchez-Escamilla, H. Elsabah, A. Fadul, E. Maffini, G. Pittari, B. Bruno, The advent of CAR T-cell therapy for lymphoproliferative neoplasms: Integrating research into clinical practice. *Front. Immunol.* **11**, 888 (2020).
2. G. Ghilardi, P. Braendstrup, E. A. Chong, S. J. Schuster, J. Svoboda, M. Ruella, CAR-T TREK through the lymphoma universe, to boldly go where no other therapy has gone before. *Br. J. Haematol.* **193**, 449–465 (2021).
3. E. A. Chong, M. Ruella, S. J. Schuster; Lymphoma Program Investigators at the University of Pennsylvania, Five-year outcomes for refractory B-cell lymphomas with CAR T-cell therapy. *N. Engl. J. Med.* **384**, 673–674 (2021).
4. S. L. Maude, T. W. Laetsch, J. Buechner, S. Rives, M. Boyer, H. Bittencourt, P. Bader, M. R. Verneris, H. E. Stefanski, G. D. Myers, M. Qayed, B. De Moerloose, H. Hiramatsu, K. Schlis, K. L. Davis, P. L. Martin, E. R. Nemecek, G. A. Yanik, C. Peters, A. Baruchel, N. Boissel, F. Mechinaud, A. Balduzzi, J. Krueger, C. H. June, B. L. Levine, P. Wood, T. Taran, M. Leung, K. T. Mueller, Y. Zhang, K. Sen, D. Lebwohl, M. A. Pulsipher, S. A. Grupp, Tisagenlecleucel in children and young adults with B-cell lymphoblastic leukemia. *N. Engl. J. Med.* **378**, 439–448 (2018).
5. J. H. Park, I. Riviere, M. Gonen, X. Wang, B. Senechal, K. J. Curran, C. Sauter, Y. Wang, B. Santomasso, E. Mead, M. Roshal, P. Maslak, M. Davila, R. J. Brentjens, M. Sadelain, Long-term follow-up of CD19 CAR therapy in acute lymphoblastic leukemia. *N. Engl. J. Med.* **378**, 449–459 (2018).
6. M. Ruella, M. V. Maus, Catch me if you can: Leukemia escape after CD19-directed T cell immunotherapies. *Comput. Struct. Biotechnol. J.* **14**, 357–362 (2016).
7. F. L. Locke, A. Ghobadi, C. A. Jacobson, D. B. Miklos, L. J. Lekakis, O. O. Oluwole, Y. Lin, I. Braunschweig, B. T. Hill, J. M. Timmerman, A. Deol, P. M. Reagan, P. Stiff, I. W. Flinn, U. Farooq, A. Goy, P. A. McSweeney, J. Munoz, T. Siddiqi, J. C. Chavez, A. F. Herrera, N. L. Bartlett, J. S. Wiezorek, L. Navale, A. Xue, Y. Jiang, A. Bot, J. M. Rossi, J. J. Kim, W. Y. Go, S. S. Neelapu, Long-term safety and activity of axicabtagene ciloleucel in refractory large B-cell lymphoma (ZUMA-1): A single-arm, multicentre, phase 1-2 trial. *Lancet Oncol.* **20**, 31–42 (2019).
8. S. J. Schuster, M. R. Bishop, C. S. Tam, E. K. Waller, P. Borchmann, J. P. McGuirk, U. Jager, S. Jaglowski, C. Andreadis, J. R. Westin, I. Fleury, V. Bachanova, S. R. Foley, P. J. Ho, S. Mielke, J. M. Magenau, H. Holte, S. Pantano, L. B. Pacaud, R. Awasthi, J. Chu, O. Anak, G. Salles, R. T. Maziarz; JULIET Investigators, Tisagenlecleucel in adult relapsed or refractory diffuse large B-cell lymphoma. *N. Engl. J. Med.* **380**, 45–56 (2019).
9. J. S. Abramson, M. L. Palomba, L. I. Gordon, M. A. Lunning, M. Wang, J. Arnason, A. Mehta, E. Purev, D. G. Maloney, C. Andreadis, A. Sehgal, S. R. Solomon, N. Ghosh, T. M. Albertson, J. Garcia, A. Kostic, M. Mallaney, K. Ogasawara, K. Newhall, Y. Kim, D. Li, T. Siddiqi, Lisocabtagene maraleucel for patients with relapsed or refractory large B-cell lymphomas (TRANSCEND NHL 001): A multicentre seamless design study. *Lancet* **396**, 839–852 (2020).
10. M. Wang, J. Munoz, A. Goy, F. L. Locke, C. A. Jacobson, B. T. Hill, J. M. Timmerman, H. Holmes, S. Jaglowski, I. W. Flinn, P. A. McSweeney, D. B. Miklos, J. M. Pagel, M. J. Kersten, N. Milpied, H. Fung, M. S. Topp, R. Houot, A. Beitinjaneh, W. Peng, L. Zheng, J. M. Rossi, R. K. Jain, A. V. Rao, P. M. Reagan, KTE-X19 CAR T-cell therapy in relapsed or refractory mantle-cell lymphoma. *N. Engl. J. Med.* **382**, 1331–1342 (2020).
11. K. Watanabe, S. Kuramitsu, A. D. Posey Jr., C. H. June, Expanding the therapeutic window for CAR T cell therapy in solid tumors: The knowns and unknowns of CAR T cell biology. *Front. Immunol.* **9**, 2486 (2018).
12. S. Mardiana, S. Gill, CAR T cells for acute myeloid leukemia: State of the art and future directions. *Front. Oncol.* **10**, 697 (2020).
13. L. C. Fleischer, H. T. Spencer, S. S. Raikar, Targeting T cell malignancies using CAR-based immunotherapy: Challenges and potential solutions. *J. Hematol. Oncol.* **12**, 141 (2019).
14. S. A. Pileri, V. Tabanelli, S. Fiori, A. Calleri, F. Melle, G. Motta, D. Lorenzini, C. Tarella, E. Derenzini, Peripheral T-cell lymphoma, not otherwise specified: Clinical manifestations, diagnosis, and future treatment. *Cancers* **13**, 4535 (2021).
15. M. G. Angelos, R. P. Patel, M. Ruella, S. K. Barta, Progress and pitfalls of chimeric antigen receptor t cell immunotherapy against T cell malignancies. *Transplant. Cell. Ther.* **30**, 171–186 (2024).
16. N. N. Shah, T. J. Fry, Mechanisms of resistance to CAR T cell therapy. *Nat. Rev. Clin. Oncol.* **16**, 372–385 (2019).
17. N. Osman, S. C. Ley, M. J. Crumpton, Evidence for an association between the T cell receptor/CD3 antigen complex and the CD5 antigen in human T lymphocytes. *Eur. J. Immunol.* **22**, 2995–3000 (1992).
18. M. Tabbekh, M. Mokrani-Hammani, G. Bismuth, F. Mami-Chouaib, T-cell modulatory properties of CD5 and its role in antitumor immune responses. *Oncoimmunology* **2**, e22841 (2013).
19. J. M. Conley, L. J. Berg, TCR signaling: It's all about the numbers. *Nat. Immunol.* **20**, 1415–1416 (2019).
20. P. Stamou, J. de Jersey, D. Carmignac, C. Mamalaki, D. Kioussis, B. Stockinger, Chronic exposure to low levels of antigen in the periphery causes reversible functional impairment correlating with changes in CD5 levels in monoclonal CD8 T cells. *J. Immunol.* **171**, 1278–1284 (2003).
21. M. Tabbekh, K. Franciszkiewicz, H. Haouas, Y. Lecluse, K. Benihoud, C. Raman, F. Mami-Chouaib, Rescue of tumor-infiltrating lymphocytes from activation-induced cell death enhances the antitumor CTL response in CD5-deficient mice. *J. Immunol.* **187**, 102–109 (2011).
22. Z. Dai, W. Mu, Y. Zhao, X. Jia, J. Liu, Q. Wei, T. Tan, J. Zhou, The rational development of CD5-targeting biepitopic CARs with fully human heavy-chain-only antigen recognition domains. *Mol. Ther.* **29**, 2707–2722 (2021).
23. J. L. Klitgaard, K. Koefoed, C. Geisler, O. V. Gadeberg, D. A. Frank, J. Petersen, J. Jurlander, M. W. Pedersen, Combination of two anti-CD5 monoclonal antibodies synergistically induces complement-dependent cytotoxicity of chronic lymphocytic leukaemia cells. *Br. J. Haematol.* **163**, 182–193 (2013).
24. M. Ruella, J. Xu, D. M. Barrett, J. A. Fraietta, T. J. Reich, D. E. Ambrose, M. Klichinsky, O. Shestova, P. R. Patel, I. Kulikovskaya, F. Nazimuddin, V. G. Bhoj, E. J. Orlando, T. J. Fry, H. Bitter, S. L. Maude, B. L. Levine, C. L. Nobles, F. D. Bushman, R. M. Young, J. Scholler, S. I. Gill, C. H. June, S. A. Grupp, S. F. Lacey, J. J. Melenhorst, Induction of resistance to chimeric antigen receptor T cell therapy by transduction of a single leukemic B cell. *Nat. Med.* **24**, 1499–1503 (2018).
25. P. Guruprasad, A.Carturan, Y. Zhang, J. H. Cho, K. G. Kumashie, R. P. Patel, K. H. Kim, J.-S. Lee, Y. Lee, J. H. Kim, J. Chung, A. Joshi, I. Cohen, M. Shestov, G. Ghilardi, J. Harris, R. Pajarillo, M. Angelos, Y. G. Lee, O. H. Ugwuanyi, S. J. A. Hong, A. C. Bochi-Layec, C. T. Sauter, L. Chen, L. Paruzzo, S. Kammerman, O. Shestova, D. Liu, L. A. Vella, S. J. Schuster, J. Svoboda, P. Porazzi, The BTLA–HVEM axis restricts CAR T cell efficacy in cancer. *Nat Immun* **25**, 1020-1032 (2024).
26. F. Marofi, R. Motavalli, V. A. Safonov, L. Thangavelu, A. V. Yumashev, M. Alexander, N. Shomali, M. S. Chartrand, Y. Pathak, M. Jarahian, S. Izadi, A. Hassanzadeh, N. Shirafkan, S. Tahmasebi, F. M. Khiavi, CAR T cells in solid tumors: Challenges and opportunities. *Stem Cell Res. Ther.* **12**, 81 (2021).
27. A. R. Haas, R. J. Golden, L. A. Litzky, B. Engels, L. Zhao, F. Xu, J. A. Taraszka, M. Ramones, B. Granda, W. J. Chang, J. Jadlowsky, K. M. Shea, A. Runkle, A. Chew, E. Dowd, V. Gonzalez, F. Chen, X. Liu, C. Fang, S. Jiang, M. M. Davis, N. C. Sheppard, Y. Zhao, J. A. Fraietta, S. F. Lacey, G. Plesa, J. J. Melenhorst, K. Mansfield, J. L. Brogdon, R. M. Young, S. M. Albelda, C. H. June, J. L. Tanyi, Two cases of severe pulmonary toxicity from highly active mesothelin-directed CAR T cells. *Mol. Ther.* **31**, 2309–2325 (2023).
28. Y. Zhao, Q. J. Wang, S. Yang, J. N. Kochenderfer, Z. Zheng, X. Zhong, M. Sadelain, Z. Eshhar, S. A. Rosenberg, R. A. Morgan, A herceptin-based chimeric antigen receptor with modified signaling domains leads to enhanced survival of transduced T lymphocytes and antitumor activity. *J. Immunol.* **183**, 5563–5574 (2009).
29. J. Eyquem, J. Mansilla-Soto, T. Giavridis, S. J. C. van der Stegen, M. Hamieh, K. M. Cunanan, A. Odak, M. Gönen, M. Sadelain, Targeting a CAR to the TRAC locus with CRISPR/Cas9 enhances tumour rejection. *Nature* **543**, 113–117 (2017).
30. G. P. Linette, M. Becker-Hapak, Z. L. Skidmore, M. L. Baroja, C. Xu, J. Hundal, D. H. Spencer, W. Fu, C. Cummins, M. Robnett, S. Kaabinejadian, W. H. Hildebrand, V. Magrini, R. Demeter, A. S. Krupnick, O. L. Griffith, M. Griffith, E. R. Mardis, B. M. Carreno, Immunological ignorance is an enabling feature of the oligo-clonal T cell response to melanoma neoantigens. *Proc. Natl. Acad. Sci. U.S.A.* **116**, 23662–23670 (2019).
31. G. Voisinne, A. Garcia-Blesa, K. Chaoui, F. Fiore, E. Bergot, L. Girard, M. Malissen, O. Burlet-Schiltz, A. Gonzalez de Peredo, B. Malissen, R. Roncagalli, Co-recruitment

analysis of the CBL and CBLB signalosomes in primary T cells identifies CD5 as a key regulator of TCR-induced ubiquitylation. *Mol. Syst. Biol.* **12**, 876 (2016).
32. G. Voisinne, K. Kersse, K. Chaoui, L. Lu, J. Chaix, L. Zhang, M. Goncalves Menoita, L. Girard, Y. Ounoughene, H. Wang, O. Burlet-Schiltz, H. Luche, F. Fiore, M. Malissen, A. Gonzalez de Peredo, Y. Liang, R. Roncagalli, B. Malissen, Quantitative interactomics in primary T cells unveils TCR signal diversification extent and dynamics. *Nat. Immunol.* **20**, 1530–1541 (2019).
33. G. Blaize, H. Daniels-Treffandier, M. Aloulou, N. Rouquie, C. Yang, M. Marcellin, M. Gador, M. Benamar, M. Ducatez, K. D. Song, O. Burlet-Schiltz, A. Saoudi, P. E. Love, N. Fazilleau, A. Gonzalez de Peredo, R. Lesourne, CD5 signalosome coordinates antagonist TCR signals to control the generation of Treg cells induced by foreign antigens. *Proc. Natl. Acad. Sci. U.S.A.* **117**, 12969–12979 (2020).
34. J. J. Perez-Villar, G. S. Whitney, M. A. Bowen, D. H. Hewgill, A. A. Aruffo, S. B. Kanner, CD5 negatively regulates the T-cell antigen receptor signal transduction pathway: Involvement of SH2-containing phosphotyrosine phosphatase SHP-1. *Mol. Cell. Biol.* **19**, 2903–2912 (1999).
35. A. Kosugi, J. Sakakura, K. Yasuda, M. Ogata, T. Hamaoka, Involvement of SHP-1 tyrosine phosphatase in TCR-mediated signaling pathways in lipid rafts. *Immunity* **14**, 669–680 (2001).
36. J. M. Conley, M. P. Gallagher, L. J. Berg, T cells and gene regulation: The switching on and turning up of genes after T cell receptor stimulation in CD8 T cells. *Front. Immunol.* **7**, 76 (2016).
37. N. A. Dower, S. L. Stang, D. A. Bottorff, J. O. Ebinu, P. Dickie, H. L. Ostergaard, J. C. Stone, RasGRP is essential for mouse thymocyte differentiation and TCR signaling. *Nat. Immunol.* **1**, 317–321 (2000).
38. J. O. Ebinu, D. A. Bottorff, E. Y. Chan, S. L. Stang, R. J. Dunn, J. C. Stone, RasGRP, a Ras guanyl nucleotide- releasing protein with calcium- and diacylglycerol-binding motifs. *Science* **280**, 1082–1086 (1998).
39. F. Alotaibi, M. Rytelewski, R. Figueredo, R. Zareardalan, M. Zhang, P. J. Ferguson, S. Maleki Vareki, Y. Najajreh, M. El-Hajjar, X. Zheng, W. P. Min, J. Koropatnick, CD5 blockade enhances ex vivo $CD8^+$ T cell activation and tumour cell cytotoxicity. *Eur. J. Immunol.* **50**, 695–704 (2020).
40. J. G. Henderson, A. Opejin, A. Jones, C. Gross, D. Hawiger, CD5 instructs extrathymic regulatory T cell development in response to self and tolerizing antigens. *Immunity* **42**, 471–483 (2015).
41. R. Yang, S. Cheng, N. Luo, R. Gao, K. Yu, B. Kang, L. Wang, Q. Zhang, Q. Fang, L. Zhang, C. Li, A. He, X. Hu, J. Peng, X. Ren, Z. Zhang, Distinct epigenetic features of tumor-reactive $CD8^+$ T cells in colorectal cancer patients revealed by genome-wide DNA methylation analysis. *Genome Biol.* **21**, 2 (2019).
42. S. Li, K. Li, F. Tian, H. Li, Q. Xia, T. Li, B. Dong, D. Li, J. Yu, J. Zhang, L. Wang, C. Zhang, S. Xu, Y. Zhao, Y. Liu, A high interferon gamma signature of CD8(+) T cells predicts response to neoadjuvant immunotherapy plus chemotherapy in gastric cancer. *Front. Immunol.* **13**, 1056144 (2022).
43. Y. L. Peng, L. B. Xiong, Z. H. Zhou, K. Ning, Z. Li, Z. S. Wu, M. H. Deng, W. S. Wei, N. Wang, X. P. Zou, Z. S. He, J. W. Huang, J. H. Luo, J. Y. Liu, N. Jia, Y. Cao, H. Han, S. J. Guo, P. Dong, C. P. Yu, F. J. Zhou, Z. L. Zhang, Single-cell transcriptomics reveals a low $CD8^+$ T cell infiltrating state mediated by fibroblasts in recurrent renal cell carcinoma. *J. Immunother. Cancer* **10**, e004206 (2022).
44. M. A. Brehm, L. L. Kenney, M. V. Wiles, B. E. Low, R. M. Tisch, L. Burzenski, C. Mueller, D. L. Greiner, L. D. Shultz, Lack of acute xenogeneic graft- versus-host disease, but retention of T-cell function following engraftment of human peripheral blood mononuclear cells in NSG mice deficient in MHC class I and II expression. *FASEB J.* **33**, 3137–3151 (2019).
45. M. Uribe-Herranz, S. Beghi, M. Ruella, K. Parvathaneni, S. Salaris, N. Kostopoulos, S. S. George, S. Pierini, E. Krimitza, F. Costabile, G. Ghilardi, K. V. Amelsberg, Y. G. Lee, R. Pajarillo, C. Markmann, B. McGettigan-Croce, D. Agarwal, N. Frey, S. F. Lacey, J. Scholler, K. Gabunia, G. Wu, E. Chong, D. L. Porter, C. H. June, S. J. Schuster, V. Bhoj, A. Facciabene, Modulation of the gut microbiota engages antigen cross-presentation to enhance antitumor effects of CAR T cell immunotherapy. *Mol. Ther.* **31**, 686–700 (2023).
46. R. K. Vaddepally, P. Kharel, R. Pandey, R. Garje, A. B. Chandra, Review of indications of FDA-approved immune checkpoint inhibitors per NCCN guidelines with the level of evidence. *Cancers (Basel)* **12**, 738 (2020).
47. E. A. Chong, C. Alanio, J. Svoboda, S. D. Nasta, D. J. Landsburg, S. F. Lacey, M. Ruella, S. Bhattacharyya, E. J. Wherry, S. J. Schuster, Pembrolizumab for B-cell lymphomas relapsing after or refractory to CD19-directed CAR T-cell therapy. *Blood* **139**, 1026–1038 (2022).
48. E. A. Stadtmauer, J. A. Fraietta, M. M. Davis, A. D. Cohen, K. L. Weber, E. Lancaster, P. A. Mangan, I. Kulikovskaya, M. Gupta, F. Chen, L. Tian, V. E. Gonzalez, J. Xu, I. Y. Jung, J. J. Melenhorst, G. Plesa, J. Shea, T. Matlawski, A. Cervini, A. L. Gaymon, S. Desjardins, A. Lamontagne, J. Salas-Mckee, A. Fesnak, D. L. Siegel, B. L. Levine, J. K. Jadlowsky, R. M. Young, A. Chew, W. T. Hwang, E. O. Hexner, B. M. Carreno, C. L. Nobles, F. D. Bushman, K. R. Parker, Y. Qi, A. T. Satpathy, H. Y. Chang, Y. Zhao, S. F. Lacey, C. H. June, CRISPR-engineered T cells in patients with refractory cancer. *Science* **367**, eaba7365 (2020).
49. C. L. Nobles, iGUIDE method for CRISPR off-target detection. *Methods Mol. Biol.* **2189**, 71–80 (2021).
50. C. L. Nobles, S. Reddy, J. Salas-McKee, X. Liu, C. H. June, J. J. Melenhorst, M. M. Davis, Y. Zhao, F. D. Bushman, iGUIDE: An improved pipeline for analyzing CRISPR cleavage specificity. *Genome Biol.* **20**, 14 (2019).
51. Z. Tang, C. Li, B. Kang, G. Gao, C. Li, Z. Zhang, GEPIA: A web server for cancer and normal gene expression profiling and interactive analyses. *Nucleic Acids Res.* **45**, W98–W102 (2017).
52. N. J. Haradhvala, M. B. Leick, K. Maurer, S. H. Gohil, R. C. Larson, N. Yao, K. M. E. Gallagher, K. Katsis, M. J. Frigault, J. Southard, S. Li, M. C. Kann, H. Silva, M. Jan, K. Rhrissorrakrai, F. Utro, C. Levovitz, R. A. Jacobs, K. Slowik, B. P. Danysh, K. J. Livak, L. Parida, J. Ferry, C. Jacobson, C. J. Wu, G. Getz, M. V. Maus, Distinct cellular dynamics associated with response to CAR-T therapy for refractory B cell lymphoma. *Nat. Med.* **28**, 1848–1859 (2022).
53. J. Pan, Y. Tan, G. Wang, B. Deng, Z. Ling, W. Song, S. Seery, Y. Zhang, S. Peng, J. Xu, J. Duan, Z. Wang, X. Yu, Q. Zheng, X. Xu, Y. Yuan, F. Yan, Z. Tian, K. Tang, J. Zhang, A. H. Chang, X. Feng, Donor-derived CD7 chimeric antigen receptor T cells for T-cell acute lymphoblastic leukemia: First-in-human, phase I trial. *J. Clin. Oncol.* **39**, 3340–3351 (2021).
54. R. Chiesa, C. Georgiadis, F. Syed, H. Zhan, A. Etuk, S. A. Gkazi, R. Preece, G. Ottaviano, T. Braybrook, J. Chu, A. Kubat, S. Adams, R. Thomas, K. Gilmour, D. O'Connor, A. Vora, W. Qasim, Base-Edited CAR T Group, Base-edited CAR7 T cells for relapsed T-cell acute lymphoblastic leukemia. *N. Engl. J. Med.* **389**, 899–910 (2023).
55. M. Mamonkin, R. H. Rouce, H. Tashiro, M. K. Brenner, A T-cell-directed chimeric antigen receptor for the selective treatment of T-cell malignancies. *Blood* **126**, 983–992 (2015).
56. M. Mamonkin, M. Mukherjee, M. Srinivasan, S. Sharma, D. Gomes-Silva, F. Mo, G. Krenciute, J. S. Orange, M. K. Brenner, Reversible transgene expression reduces fratricide and permits 4-1BB costimulation of CAR T cells directed to T-cell malignancies. *Cancer Immunol. Res.* **6**, 47–58 (2018).
57. L. C. Hill, R. H. Rouce, M. J. Wu, T. Wang, R. Ma, H. Zhang, B. Mehta, N. Lapteva, Z. Mei, T. S. Smith, L. Yang, M. Srinivasan, P. M. Burkhardt, C. A. Ramos, P. Lulla, M. Arredondo, B. Grilley, H. E. Heslop, M. K. Brenner, M. Mamonkin, Antitumor efficacy and safety of unedited autologous CD5.CAR T cells in relapsed/refractory mature T-cell lymphomas. *Blood* **143**, 1231–1241 (2024).
58. Y. Yang, R. Murray, A. Camblin, F. Musenge, L. Coholan, M. Naniong, D. Sweezy, S. Haskett, L. Young, Y. Zhang, A. Costa, H. Wu, A. Ladd, L. Barrera, L. Schlehuber, S. Smith, Y.-C. Poh, G. Ciaramella, J. Gehrke, CD5 knockout enhances the potency of multiplex base-edited allogeneic anti-CD5 CAR T-cell therapy for the treatment of T-cell malignancies. *J. Immunother. Cancer* **9**, A165 (2021).
59. S. Agarwal, M. A. Aznar, A. J. Rech, C. R. Good, S. Kuramitsu, T. Da, M. Gohil, L. Chen, S. A. Hong, P. Ravikumar, A. K. Rennels, J. Salas-Mckee, W. Kong, M. Ruella, M. M. Davis, G. Plesa, J. A. Fraietta, D. L. Porter, R. M. Young, C. H. June, Deletion of the inhibitory co-receptor CTLA-4 enhances and invigorates chimeric antigen receptor T cells. *Immunity* **56**, 2388–2407.e9 (2023).
60. J. Wei, C. Luo, Y. Wang, Y. Guo, H. Dai, C. Tong, D. Ti, Z. Wu, W. Han, PD-1 silencing impairs the anti-tumor function of chimeric antigen receptor modified T cells by inhibiting proliferation activity. *J. Immunother. Cancer* **7**, 209 (2019).
61. J. Carnevale, E. Shifrut, N. Kale, W. A. Nyberg, F. Blaeschke, Y. Y. Chen, Z. Li, S. P. Bapat, M. E. Diolaiti, P. O'Leary, S. Vedova, J. Belk, B. Daniel, T. L. Roth, S. Bachl, A. A. Anido, B. Prinzing, J. Ibanez-Vega, S. Lange, D. Haydar, M. Luetke-Eversloh, M. Born-Bony, B. Hegde, S. Kogan, T. Feuchtinger, H. Okada, A. T. Satpathy, K. Shannon, S. Gottschalk, J. Eyquem, G. Krenciute, A. Ashworth, A. Marson, RASA2 ablation in T cells boosts antigen sensitivity and long-term function. *Nature* **609**, 174–182 (2022).
62. M. W. LaFleur, T. H. Nguyen, M. A. Coxe, B. C. Miller, K. B. Yates, J. E. Gillis, D. R. Sen, E. F. Gaudiano, R. Al Abosy, G. J. Freeman, W. N. Haining, A. H. Sharpe, PTPN2 regulates the generation of exhausted $CD8^+$ T cell subpopulations and restrains tumor immunity. *Nat. Immunol.* **20**, 1335–1347 (2019).
63. J. A. Fraietta, C. L. Nobles, M. A. Sammons, S. Lundh, S. A. Carty, T. J. Reich, A. P. Cogdill, J. J. D. Morrissette, J. E. DeNizio, S. Reddy, Y. Hwang, M. Gohil, I. Kulikovskaya, F. Nazimuddin, M. Gupta, F. Chen, J. K. Everett, K. A. Alexander, E. Lin-Shiao, M. H. Gee, X. Liu, R. M. Young, D. Ambrose, Y. Wang, J. Xu, M. S. Jordan, K. T. Marcucci, B. L. Levine, K. C. Garcia, Y. Zhao, M. Kalos, D. L. Porter, R. M. Kohli, S. F. Lacey, S. L. Berger, F. D. Bushman, C. H. June, J. J. Melenhorst, Disruption of TET2 promotes the therapeutic efficacy of CD19-targeted T cells. *Nature* **558**, 307–312 (2018).
64. J. Liu, G. Zhou, L. Zhang, Q. Zhao, Building potent chimeric antigen receptor T cells with CRISPR genome editing. *Front. Immunol.* **10**, 456 (2019).
65. N. Singh, J. Shi, C. H. June, M. Ruella, Genome-editing technologies in adoptive T cell immunotherapy for cancer. *Curr. Hematol. Malig. Rep.* **12**, 522–529 (2017).
66. J. S. Sherkow, CRISPR, patents, and the public health. *Yale J. Biol. Med.* **90**, 667–672 (2017).

67. M. Kosicki, K. Tomberg, A. Bradley, Repair of double-strand breaks induced by CRISPR-Cas9 leads to large deletions and complex rearrangements. *Nat. Biotechnol.* **36**, 765–771 (2018).
68. C. A. Tsuchida, N. Brandes, R. Bueno, M. Trinidad, T. Mazumder, B. Yu, B. Hwang, C. Chang, J. Liu, Y. Sun, C. R. Hopkins, K. R. Parker, Y. Qi, L. Hofman, A. T. Satpathy, E. A. Stadtmauer, J. H. D. Cate, J. Eyquem, J. A. Fraietta, C. H. June, H. Y. Chang, C. J. Ye, J. A. Doudna, Mitigation of chromosome loss in clinical CRISPR-Cas9-engineered T cells. *Cell* **186**, 4567–4582.e20 (2023).
69. S. Ravel, M. Colombatti, P. Casellas, Internalization and intracellular fate of anti-CD5 monoclonal antibody and anti-CD5 ricin A-chain immunotoxin in human leukemic T cells. *Blood* **79**, 1511–1517 (1992).
70. X. Lu, R. C. Axtell, J. F. Collawn, A. Gibson, L. B. Justement, C. Raman, AP2 adaptor complex-dependent internalization of CD5: Differential regulation in T and B cells. *J. Immunol.* **168**, 5612–5620 (2002).
71. G. Porro, P. Lento, F. Marcucci, G. Gromo, D. Modena, Different cytotoxic activity and intracellular fate of an anti-CD5-momordin immunotoxin in normal compared to tumour cells. *Cancer Immunol. Immunother.* **40**, 213–218 (1995).

Acknowledgments: We thank L. Chen, M. Eldabbas, and E. Maddox of the Human Immunology Core at the Perelman School of Medicine at the University of Pennsylvania (NIH P30 AI045008 and P30 CA016520; HIC RRID: SCR_022380). We would also like to acknowledge the University Laboratory Animal Resources, the Cell and Animal Radiation Core (RRID: SCR_022377), the Stem Cell Xenograft Core (RRID: SCR_010035), the Flow Cytometry Core, the Next-Generation Sequencing Core, the Comparative Pathology Core, and the Viral/Molecular High Density Sequencing Core at the University of Pennsylvania for services. Portions of Figs. 1, 4, and 7 and figs. S2 and S5 were created with BioRender.com (agreement number: XU26WLFKBH). **Funding:** This work was funded through the NIH /National Cancer Institute (R37-CA-262362-02), the Leukemia and Lymphoma Society, the Gilead Research Scholar Award in Hematology, the Emerson Collective, the Laffey-McHugh Foundation, the Parker Institute for Cancer Immunotherapy, the Berman and Maguire Funds for Lymphoma Research at Penn, and viTToria Biotherapeutics (M.R.). This work was also funded through the T32 Hematology Research Training Program and the American Society of Hematology Graduate Award (R.P.P.).

Author contributions: R.P.P. planned and executed the experiments, analyzed the data, prepared the figures, conceptualized the study, and wrote the manuscript. G.G., Y.Z., Y.-H.C., W.X., P.G., K.H.K., I. Chun, M.G.A., R.P., S.J.H., Y.G.L., O.S., C.S., I. Cohen, A.G., T.V., D.Q., S.Y., A.N., A.R., O.U., M. Wang, M. Wysocka, A.C., T.B., C.X., K.G., and P.P. contributed to executing or analyzing both in vitro and in vivo experiments. Their contributions spanned DNA preparation, lentiviral production, CAR T cell expansion, conducting killing assays, and monitoring animals for tumor burden and blood processing and more. A.I. and J.H. contributed to the analysis and interpretation of tissue toxicity data. L.C. contributed by processing large single-cell sequencing datasets. G.G. and P.G. further contributed to preparing figures for publication. A.E.S., N.S., L.P., H.J.B., M.A.M., M. Wang, M. Wysocka, G.P.L., B.C., D.M.B., D.T.T., A.D.P., D.J.P.J., C.T.S., S.P., V.P., J.S., A.H.R., S.J.S., and S.K.B. provided essential resources, including materials and experimental/analytical support throughout the project. R.P.P. and M.R. acquired funding for this research. M.R. contributed in conceptualizing the study, contributing to the manuscript's writing, and supervising the study. **Competing interests:** The patent, titled "Use of cd2/5/7 knock-out anti-cd2/5/7 chimeric antigen receptor T cells against T cell lymphomas and leukemias," has been filed with M.R., A.D.P., and D.J.P.J. listed as coinventors, with the filing number WO2020132327A1. The patent, titled "Methods of manufacturing T cells," has been filed with M.R. and N.S. listed as coinventors, with the filing number PCT/US2024/031950. The patent, titled "CD5 modified cells comprising chimeric antigen receptors (CARs) for treatment of solid tumors," has been filed with M.R. listed as the inventor, with the filing number PCT/US2022/081463. M.R. holds multiple patents related to CAR T immunotherapy that are managed by the University of Pennsylvania. M.R. has served as a consultant for NanoString, BMS, GSK, Bayer, and AbClon. M.R. receives research funding from AbClon, Beckman Coulter, and Oxford Nanoimaging. M.R. is the scientific founder of viTToria Biotherapeutics. R.P.P. and G.G. receive honoraria for consulting at viTToria Biotherapeutics. T.V., D.Q., S.Y., A.N., A.E.S., and N.S. are employees of viTToria Biotherapeutics. N.S. is a cofounder and a member of the board of directors of viTToria Biotherapeutics. D.T.T. has patents and patents pending related to CAR T. D.T.T. serves on advisory boards for Beam Therapeutics, Sobi, Jazz, and Servier. D.T.T. receives research funding from Beam Therapeutics and NeoImmuneTech. S.P. has served as Diatech Pharmacogenetics scientific board president and has served as bureau speaker for Lilly, BeiGene, Takeda, Stemline, Kyowa Kirin, Roche, and NanoString. S.K.B. has served as a consultant to Acrotech, Affimed, Daiichi Sankyo, Kyowa Kirin, and Daiichi Sankyo and receives honoraria for participation in an independent data monitoring committee by J&J. S.J.S. serves on the scientific advisory boards for viTToria Biotherapeutics and Caribou Biosciences. S.J.S. has received honoraria for consulting for Kite Therapeutics, Legend Biotech, Mustang Biotech, Janssen, and Novartis. S.J.S. holds multiple patents related to CAR T immunotherapy that are managed by the University of Pennsylvania. All other authors declare no competing interests.
Data and materials availability: All requests for raw and analyzed preclinical data and materials are promptly reviewed by the University of Pennsylvania to determine whether they are subject to intellectual property or confidentiality obligations. Any data and materials that can be shared will be released via a material transfer agreement. Bulk RNA sequencing data are available from the Gene Expression Omnibus using the accession number GSE237805. Single-cell RNA sequencing data are available from the Gene Expression Omnibus using the accession number GSE248590. Raw data and full protein immunoblots are included in data files S1 and S2, respectively.

Submitted 20 December 2023
Resubmitted 11 April 2024
Accepted 26 June 2024
Published 19 July 2024
10.1126/sciimmunol.adn6509